SOTANCP4 2018, Galveston, Texas, USA

Study of Clustering in $^{17,18}O$ via Helium Decays of the Excited States

Neven Soić
Ruđer Bošković Institute Zagreb, Croatia

Collaborators

L. Prepolec, L. Grassi, D. Jelavić Malenica, T. Mijatović, S. Szilner, V. Tokić, M. Uroić
Ruđer Bošković Institute, Zagreb, Croatia

M. Milin
Faculty of Science, University of Zagreb, Croatia

M. Freer, N. I. Ashwood, Tz. Kokalova, C. Wheldon
School of Physics and Astronomy, University of Birmingham, Edgbaston, Birmingham, UK

N. L. Achouri, F. Delaunay, J. Gibelin, F. M. Marqués, N. A. Orr
Laboratoire de Physique Corpusculaire ISMRA and Université de Caen IN2P3-CNRS, Caen, France

F. Haas
Université de Strasbourg, IN2P3-CNRS Institute Pluridisciplinaire Hubert Curien, Strasbourg, France

M. Fisichella, A. Di Pietro, P. Figuera, M. Lattuada, V. Scuderi
INFN –Laboratori Nazionali del Sud, Catania, Italy

- Advantages of light nuclei
- small number of degrees of freedom
- low density of states at moderate excitations
- tests of basic principles of nuclear structure and interaction starting from individual nucleons
- structure & reactions: single particle – correlated pairs – clusters
- experimentally found p and n drip lines
- reachness of unusall nuclear configurations: clusters, Borromean (3 and 4 component systems), skin, halo, molecules

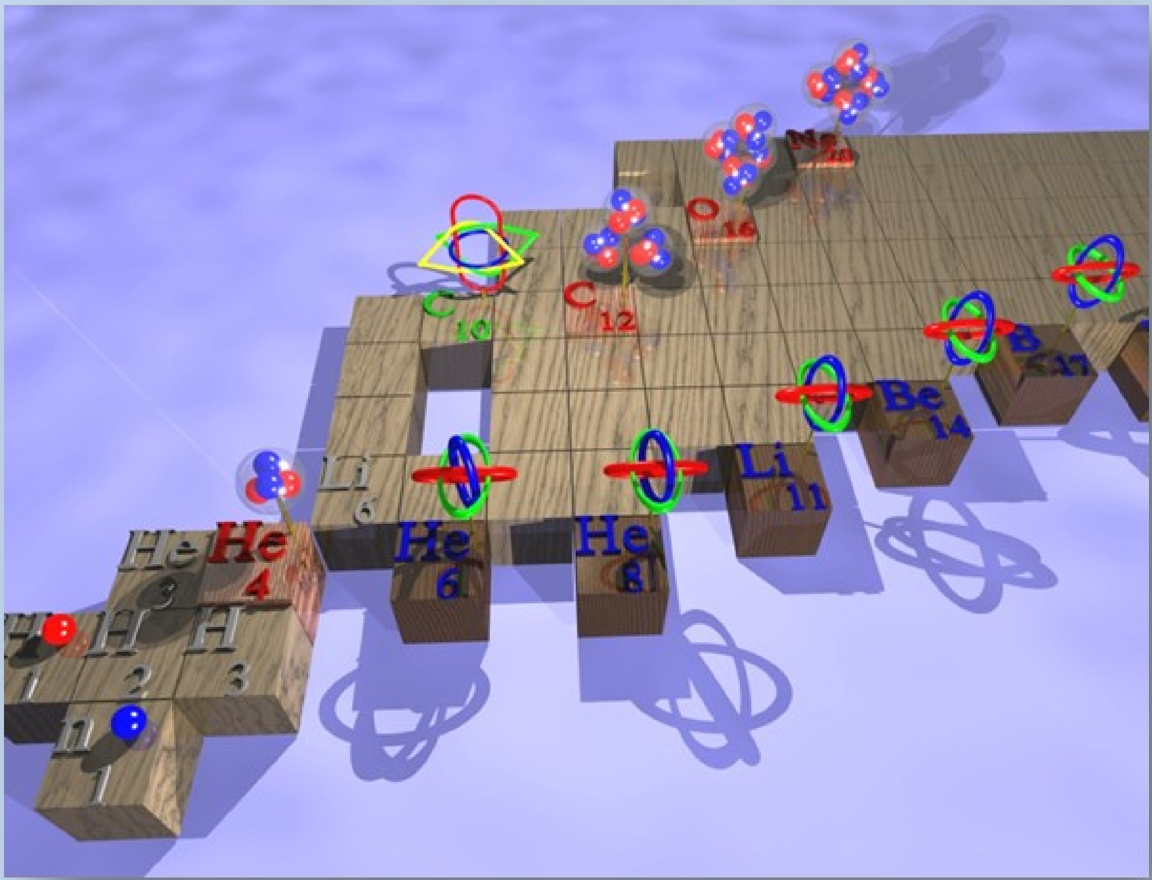

Nuclear molecules

valence neutrons exchanged between the cores

^{9,10,12}Be, ^{14,16}C, ^{18,20,22}O, ^{22,24,26}Ne

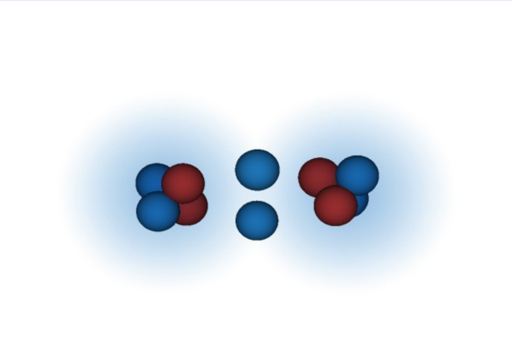

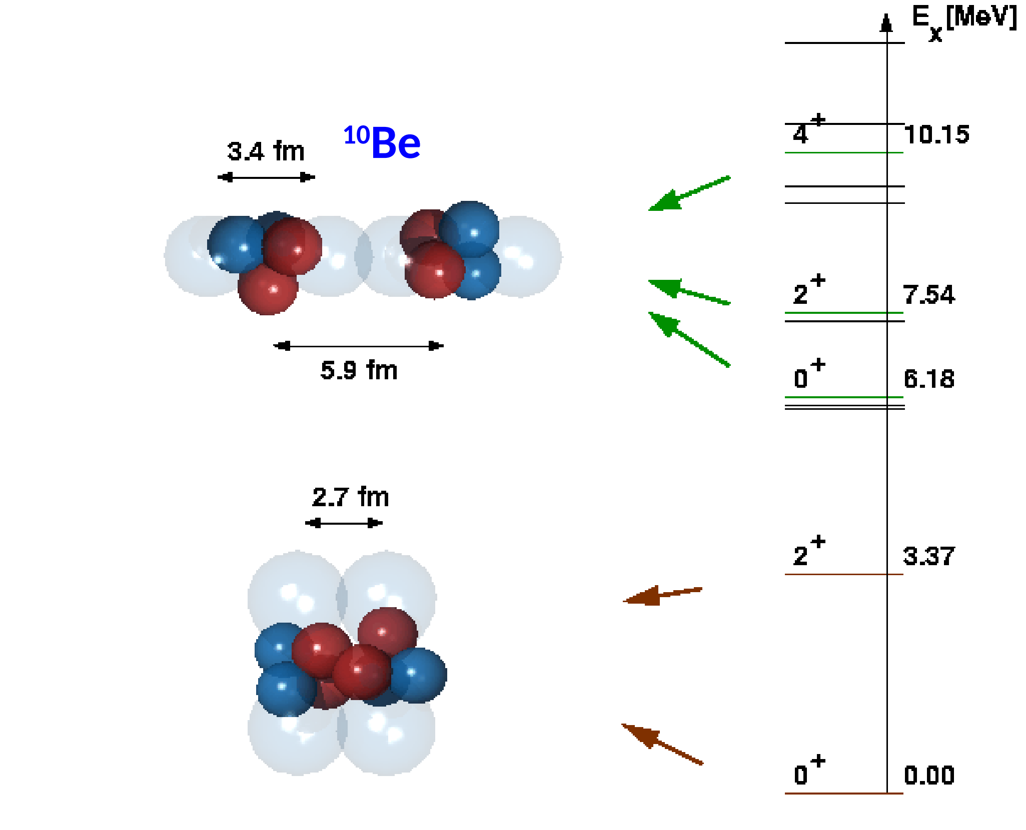

Decay by ^{6}He emission: ^{10,12}Be signature of exotic structure - molecular structure

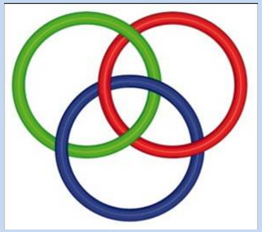

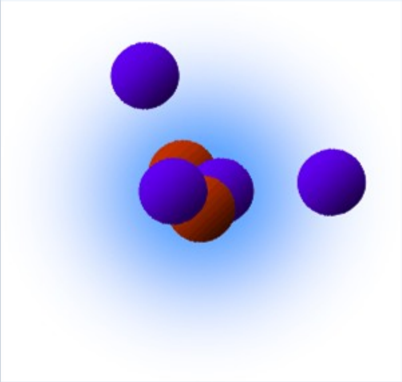

Borromean system
neutron halo

N.Soić *et al*, Europhys.Lett. (1995)

M.Milin *et al*, Europhys.Lett. (1999)

M.Milin *et al*, Nucl.Phys. (2005)

M.Freer *et al*, Phys.Rev.Lett. (2006)

Oxygen isotopes

^{16}O: double magic ground state, 1st excited state ^{12}C+α cluster structure, likely 4α cluster structure at high excitations

$K^{\pi} = 0^{+}$ rotational band

J^{π}	E_x MeV
0^{+}	6.05
2^{+}	6.92
4^{+}	10.36
6^{+}	16.28

$K^{\pi} = 0^{-}$ rotational band

J^{π}	E_x MeV
1^{-}	9.59
3^{-}	11.60
5^{-}	14.66
7^{-}	20.86

Plot of the 4p-nh states for the $^{16-18}$O

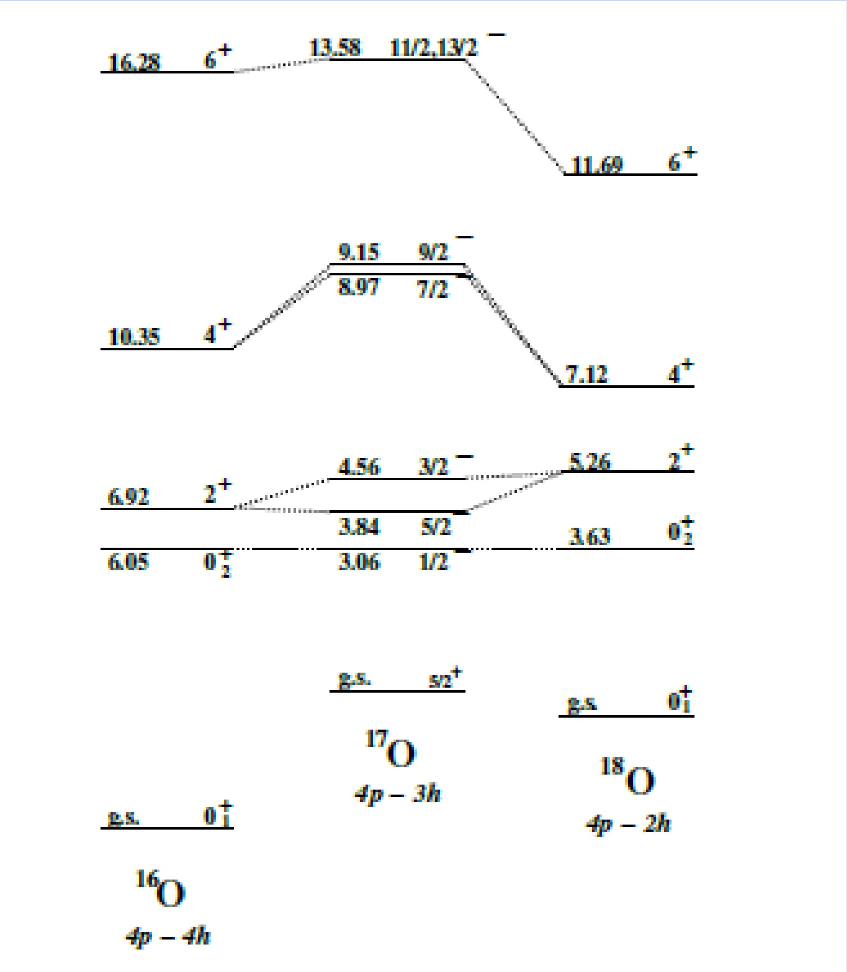

^{18}O proposed cluster configurations
W. von Oertzen et al, Eur. Phys. J. A 43 (2010) 17

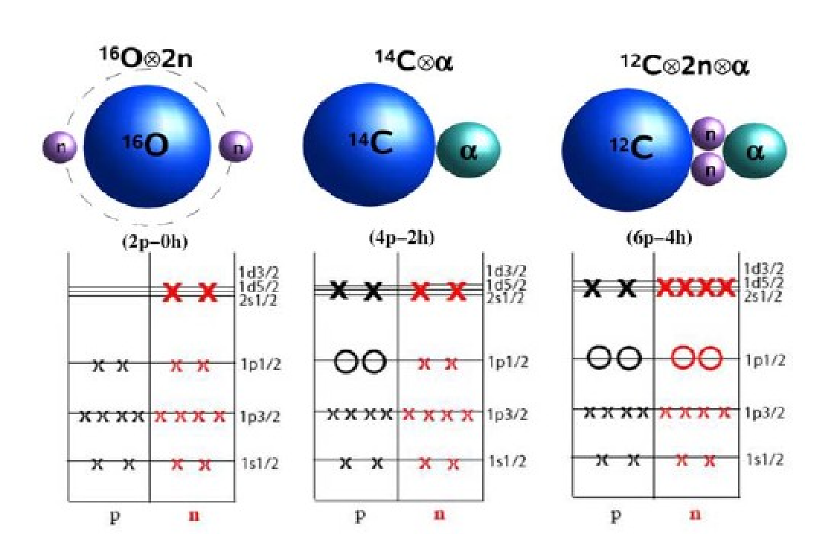

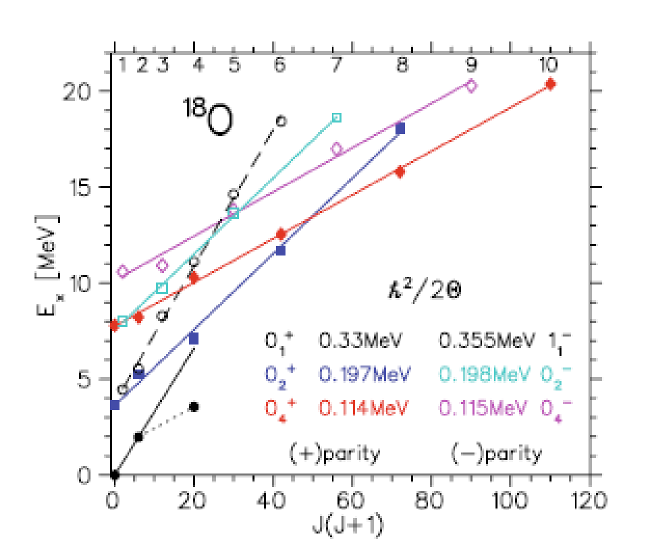

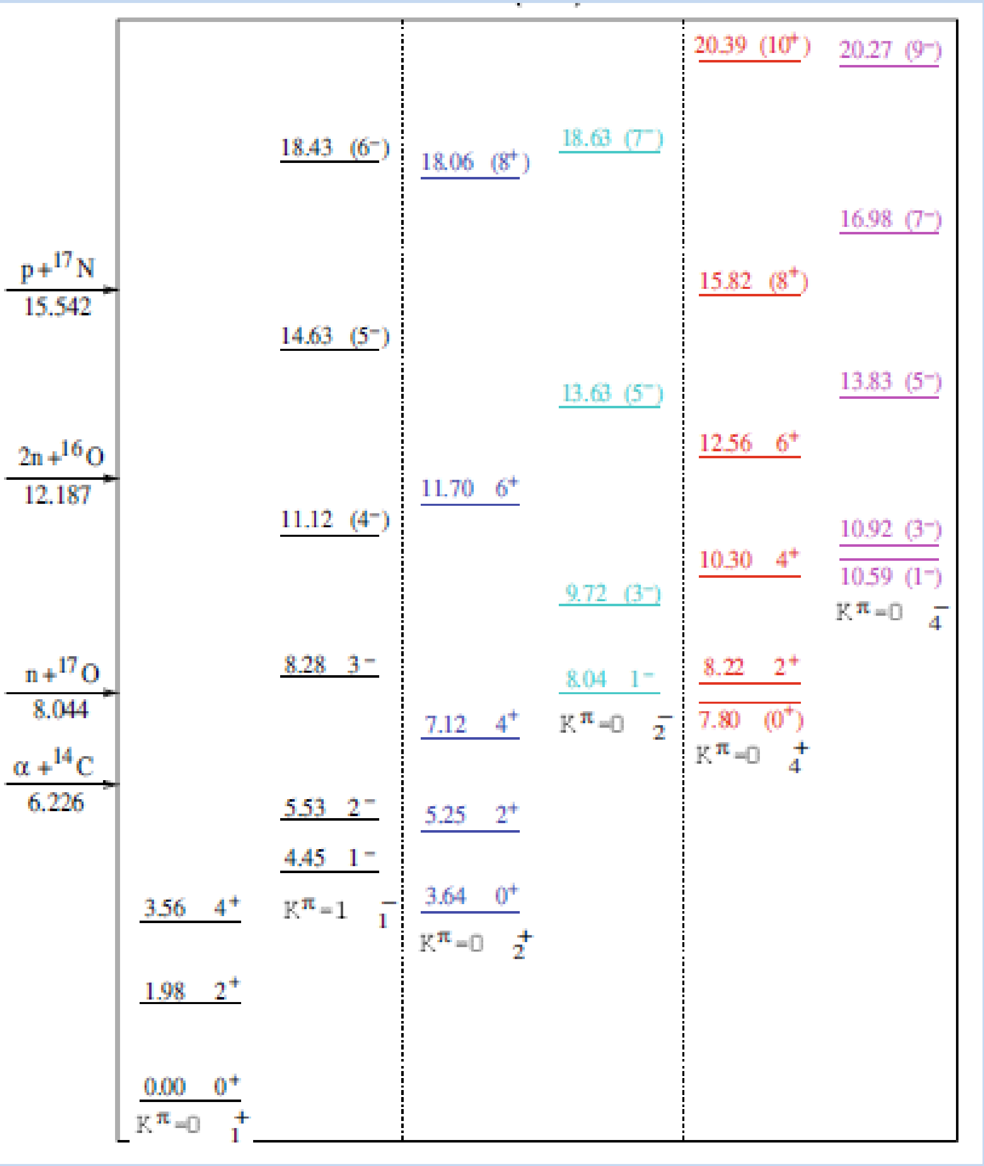

Experiment: Tandem RBI Zagreb Croatia (^{17}O)

^{13}C+^{4}He thick target resonant scattering

$E_{^{13}C}$ [MeV]	$p_{^4He}$ [mbar]	Inelastic-free $E_x(^{17}O)$ range	Run numbers
20.00	312	7.977 – 11.066	25
25.00	461	9.154 – 12.243	27
30.00	591 , 589 , 587	10.331 – 13.420	28-30, 32
33.00	699	11.037 – 14.126	33
35.00	720	11.508 – 14.597	35

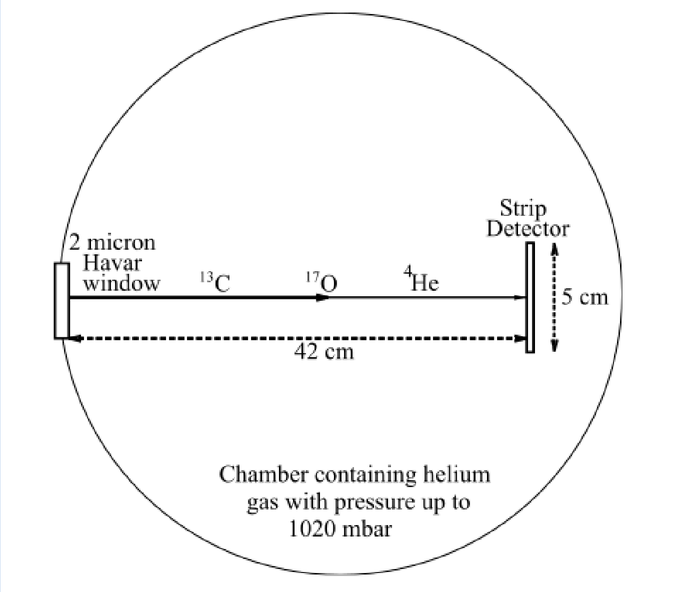

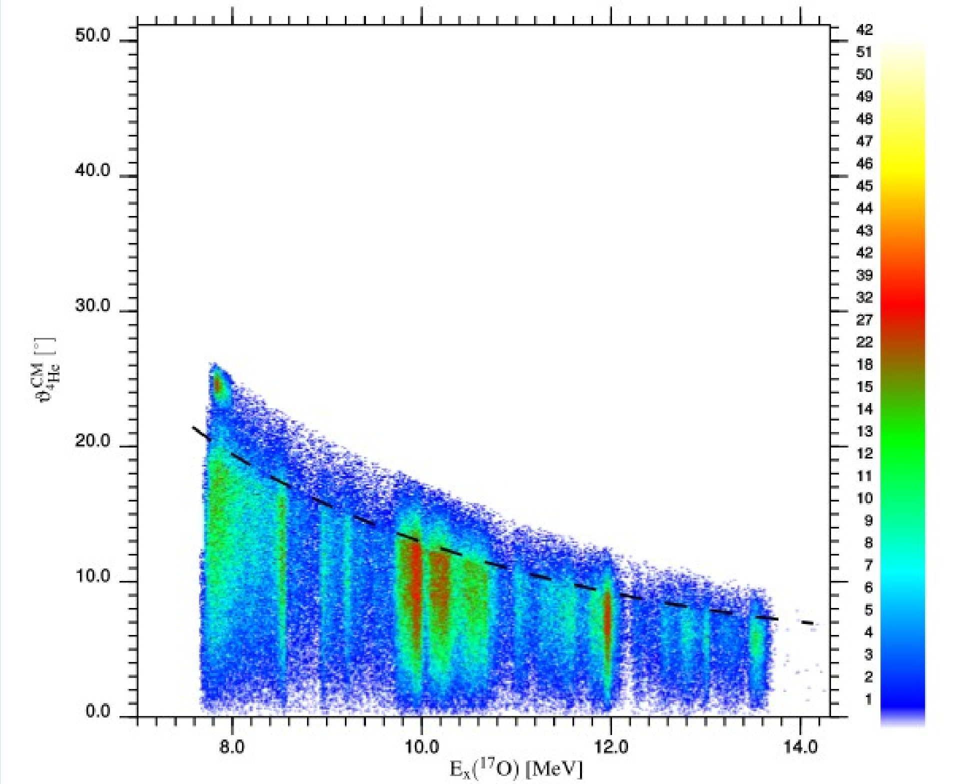

CM angle of scattered ^{4}He vs. $E_x(^{17}O)$

Assumed elastic scattering

Further steps: detection efficiency correction (Θ_{CM} < 5 deg), normalization, data averaging for different runs consistent sets of data, inelastic contribution negligible

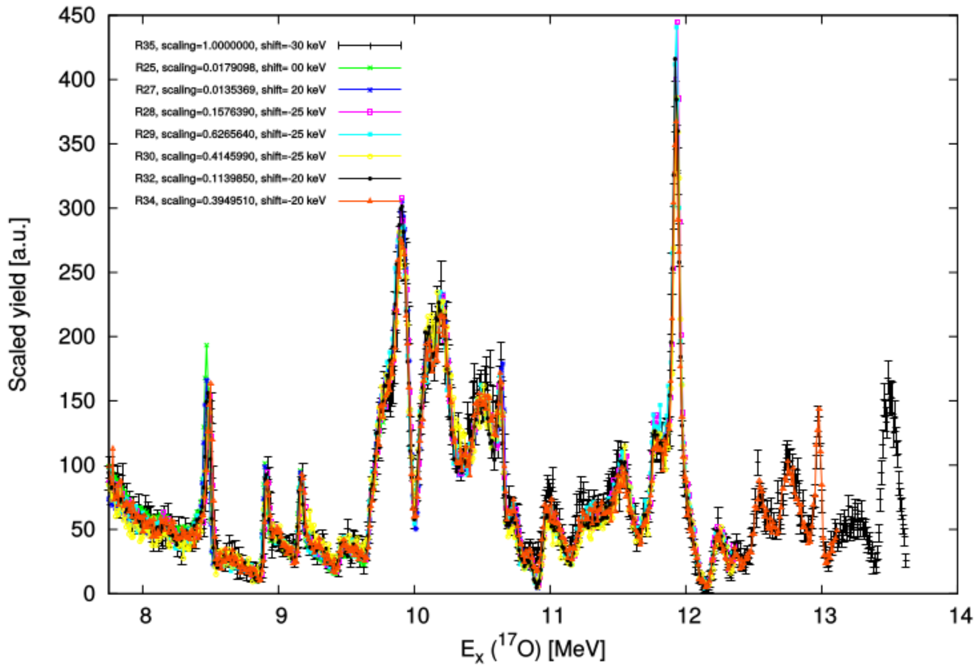

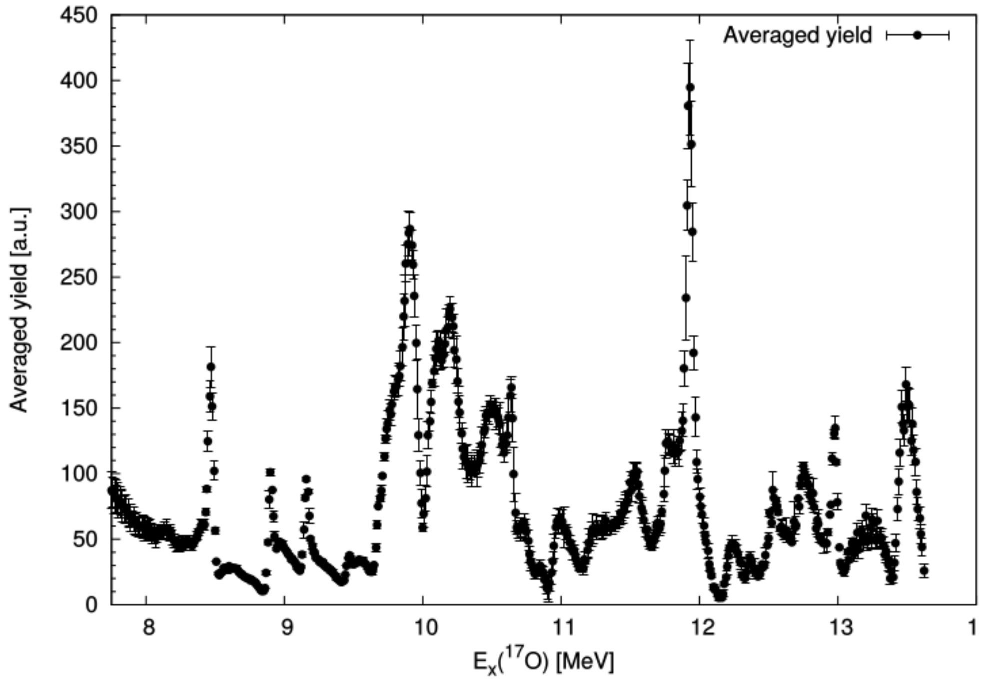

Published data: M Heil et al, PRC 78 (2008) 025803, up to excitation of 11.5 MeV
Our data at 175 deg

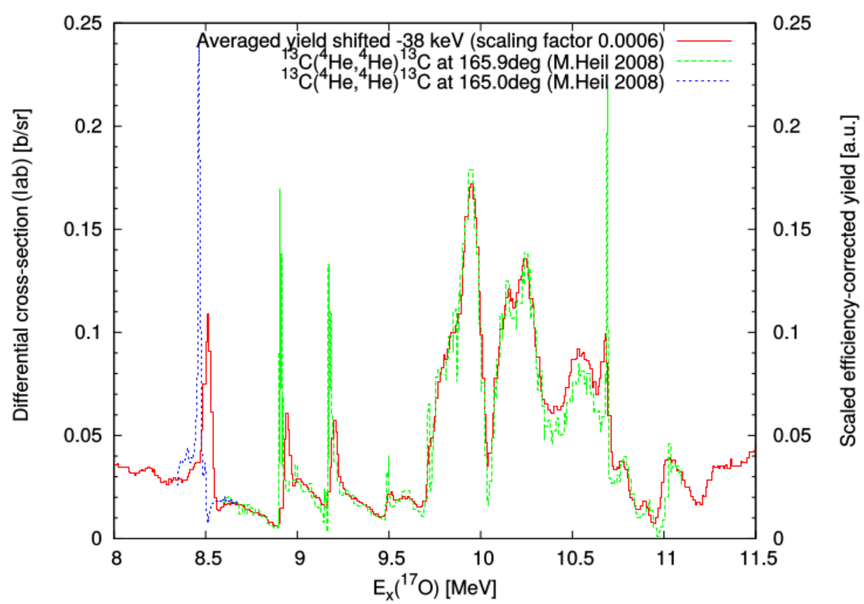

- R-matrix fits using code AZURE2 with resonance parameters from M. Heil et all (70 resonances at excitations 4.55 – 15.44 MeV obtained using code SAMMY)
- extensive fits of all available data for $^{13}C+^{4}He$ elastic scattering at number of angles, elastic and inelastic (1st and 2nd excited state) $^{16}O+n$ scattering, $^{13}C(^{4}He,n)$ reaction, $^{16}O(n,^{4}He)$ reaction
- significant discrepancies between fits and experimental results even for Heil data

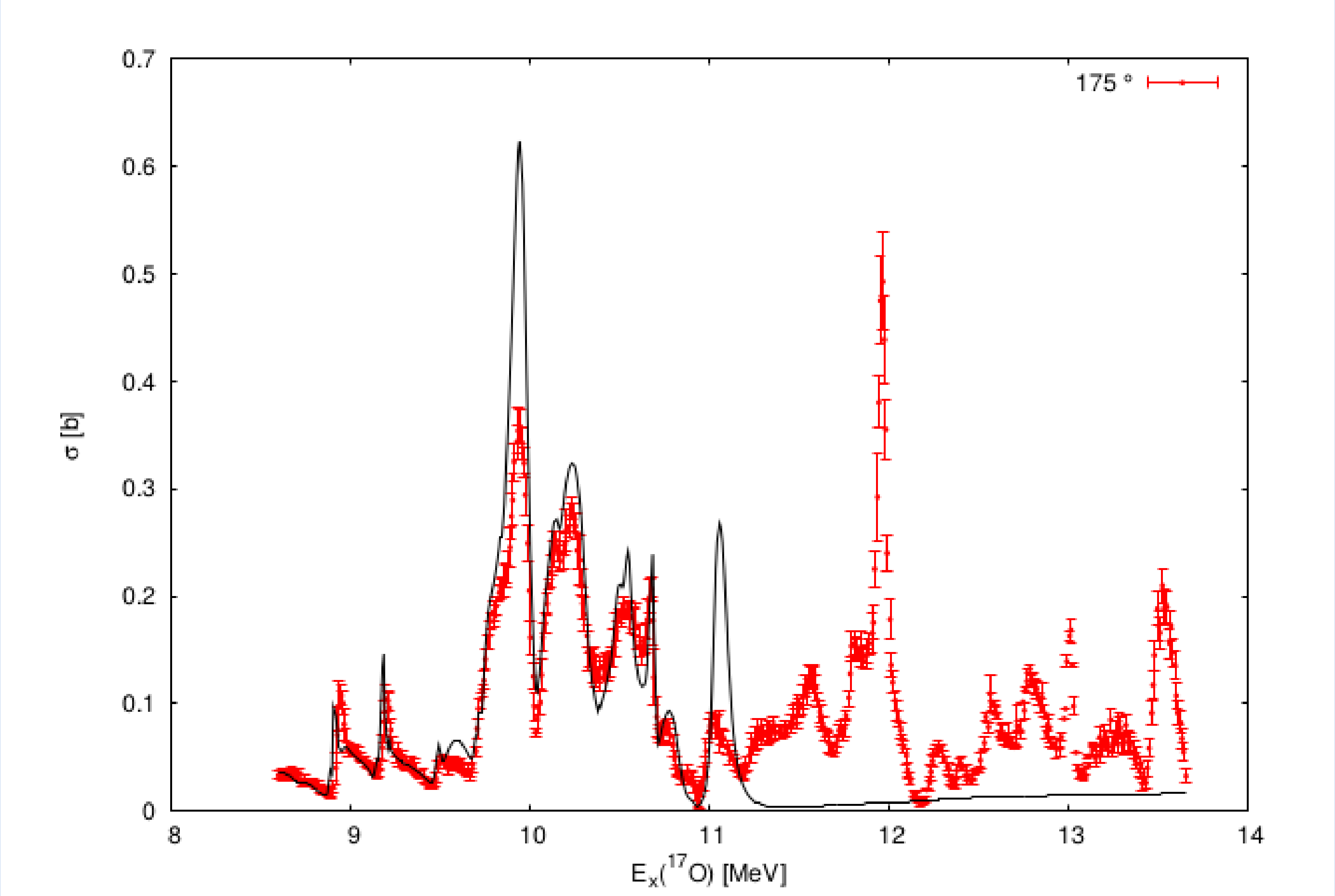

Our results for $^{13}C+^{4}He$ elastic scattering with R-matrix fit using published resonance parameters

Simplified R-matrix fit: single isolated resonance for single channel and single data set at one angle

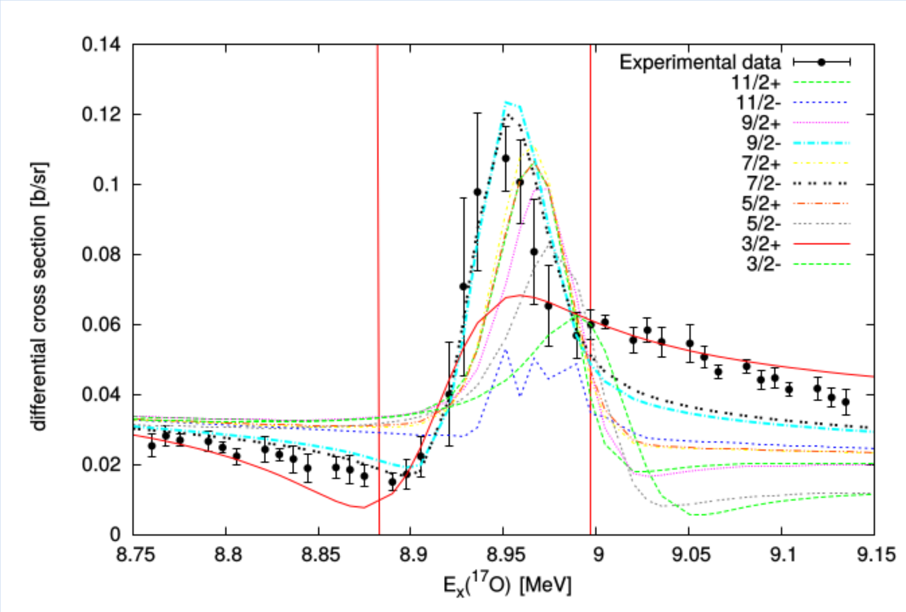

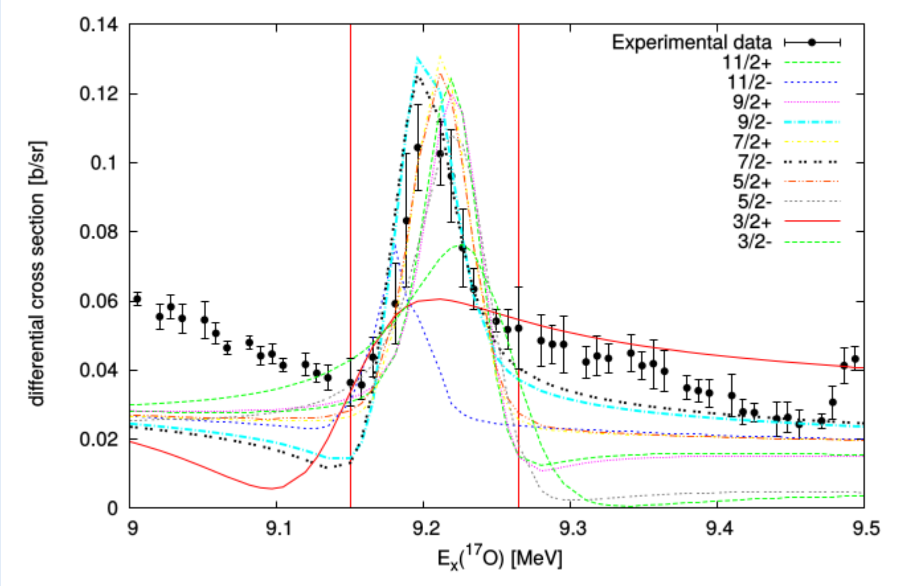

Test fits

	Peak			
	8.9 MeV		9.2 MeV	
J^π	γ [MeV$^{1/2}$]	θ_W^2	γ [MeV$^{1/2}$]	θ_W^2
$\frac{9}{2}^-$	−0.482501	0.307	0.408232	0.220
$\frac{7}{2}^-$	−0.632510	0.528	0.538238	0.382

Heil et al results

J^π	$E_x(^{17}O)$ [MeV]	Γ_n [keV]	Γ_α [keV]
$\frac{9}{2}^-$	8.9029	$-2.3 \cdot 10^{-5}$	−0.45
$\frac{7}{2}^-$	9.1737	0.038	3.26

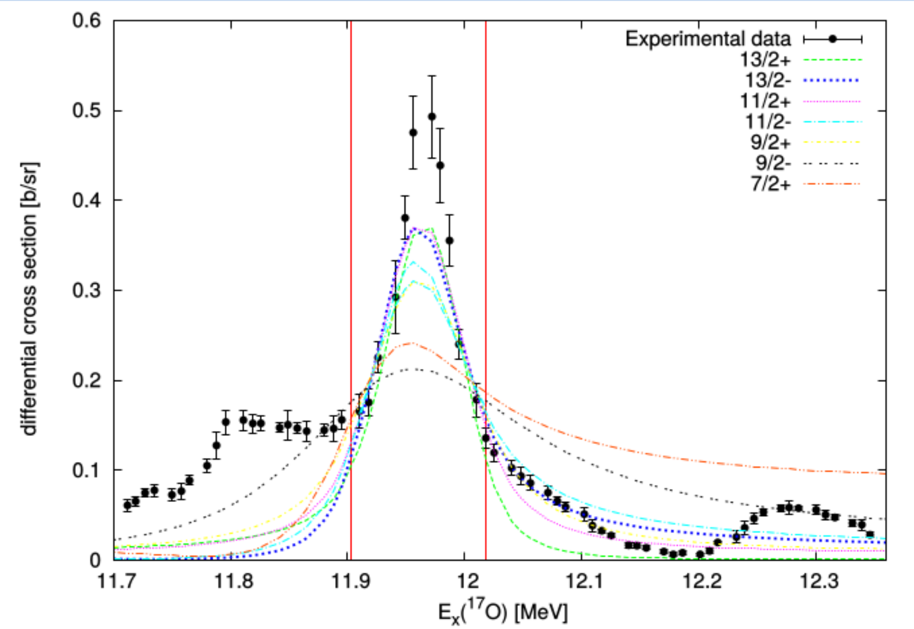

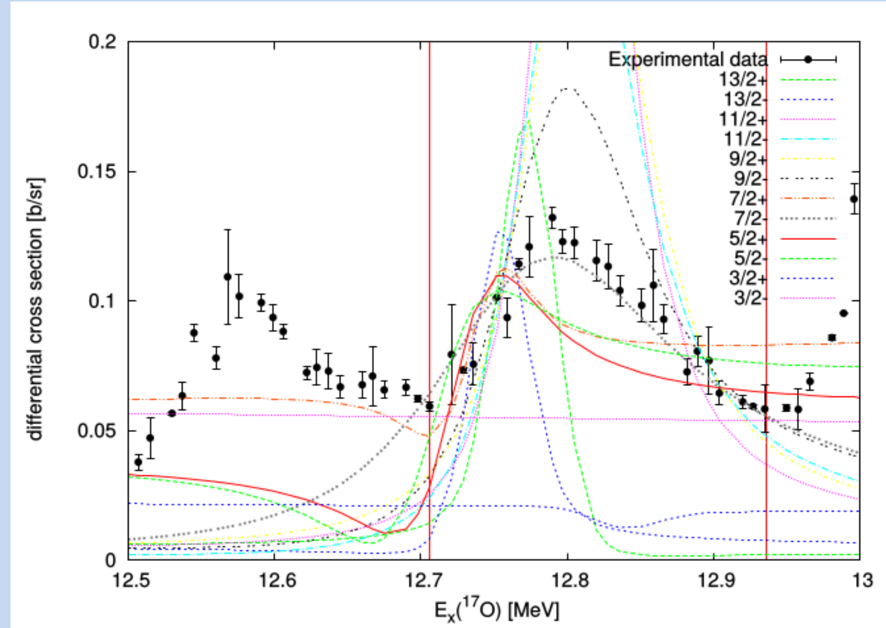

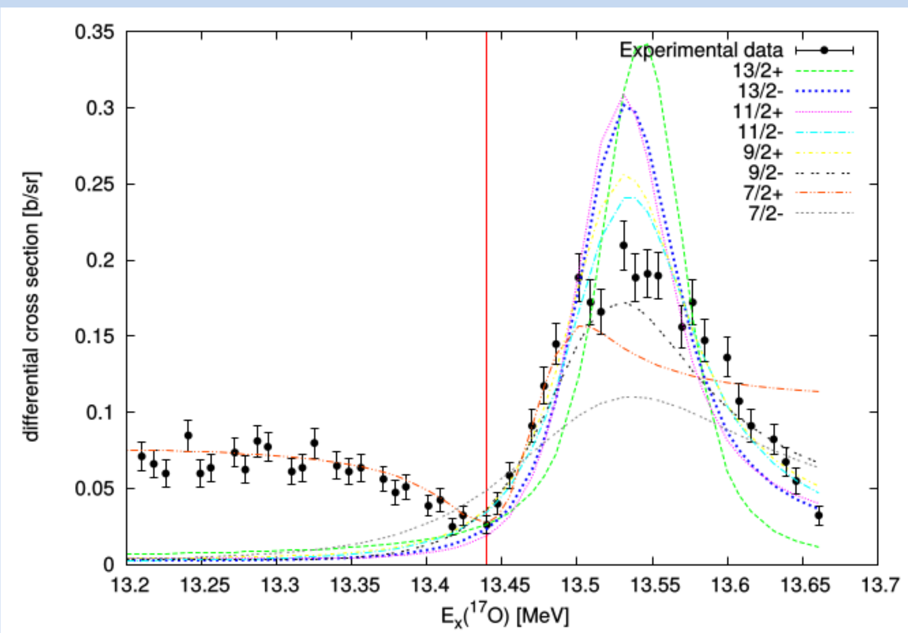

Peak								
12.0 MeV			12.8 MeV			13.6 MeV		
J^π	γ [MeV$^{1/2}$]	θ_W^2	J^π	γ [MeV$^{1/2}$]	θ_W^2	J^π	γ [MeV$^{1/2}$]	θ_W^2
$\frac{11}{2}^+$	0.339962	0.153	$\frac{7}{2}^-$	0.284347	0.107	$\frac{11}{2}^-$	0.431423	0.246
$\frac{13}{2}^-$	0.837051	0.925						

Experiment: Tandem IPN Orsay France ($^{17,18}O$)

Kinematically complete measurements - coincidences 2 of 3 reaction products

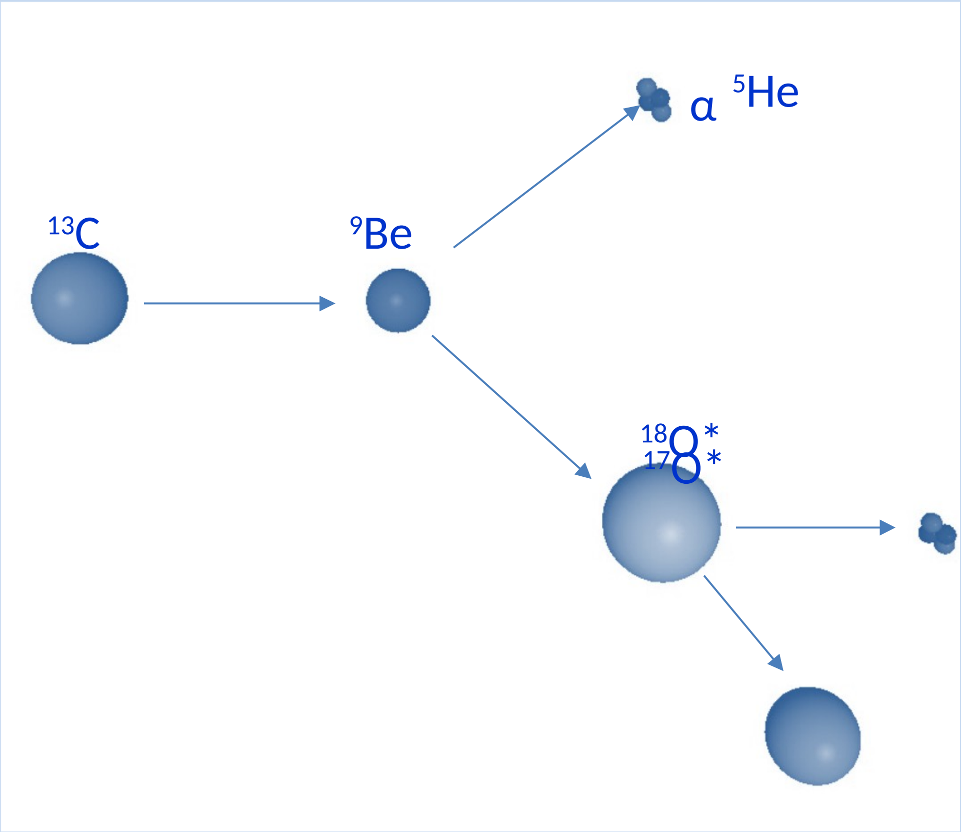

$^{13}C + ^{9}Be \rightarrow ^{5}He + ^{17}O^*$

$^{17}O^* \rightarrow \alpha + ^{13}C$, Q = -2.406 MeV

$E_{thr}(\alpha + ^{13}C)$ = 6.361 MeV

$^{13}C + ^{9}Be \rightarrow \alpha + ^{18}O^*$

$^{18}O^* \rightarrow \alpha + ^{14}C$, Q = 6.604 MeV

$^{18}O^* \rightarrow ^{6}He + ^{12}C$, Q = -5.549 MeV

$E_{thr}(\alpha + ^{14}C)$ = 6.228 MeV

$E_{thr}(^{6}He + ^{12}C)$ = 18.380 MeV

Goal: characterization of the $^{17,18}O$ resonances decaying by helium emission in excitation energy range 7 - 25 MeV: excitation energy, widths

E(^{13}C)$_{beam}$=72 MeV, ^{9}Be target thickness 100 μg/cm^{2}

6 telescopes 20 μm SSSD + 1000 DSSSD μm, 50x50 mm^{2}

Micron Semiconductor type W1

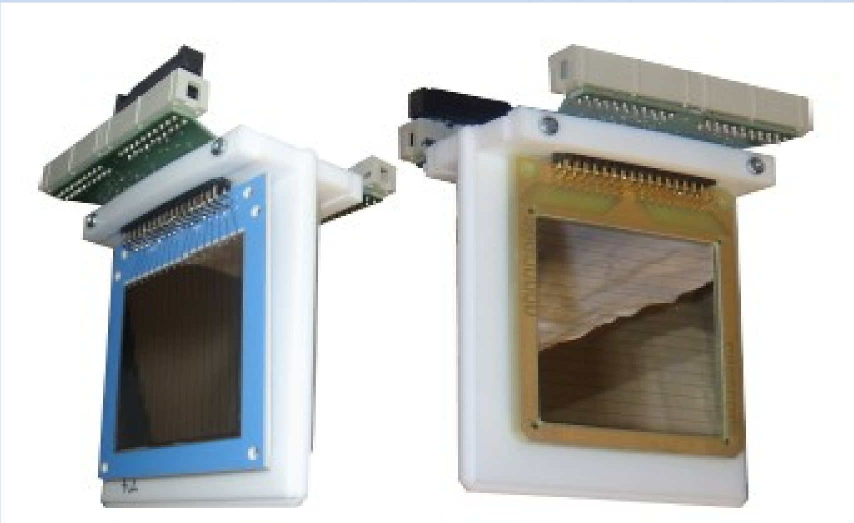

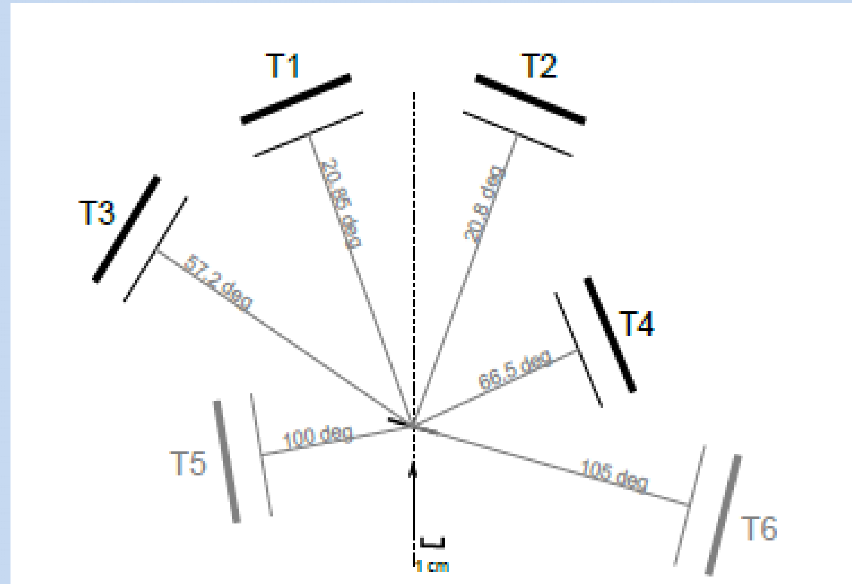

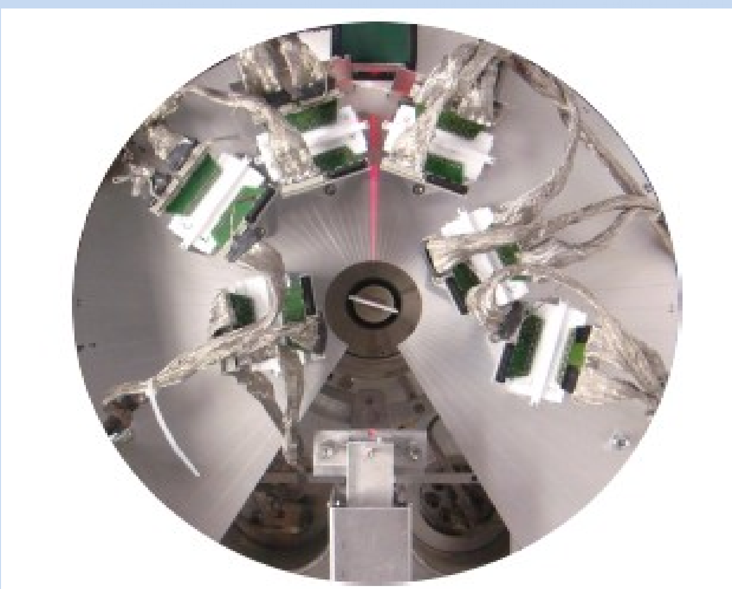

Detector telescope	$\vartheta_{min}^{in\ plane}$ [°]	$\vartheta_{max}^{in\ plane}$ [°]	$\Delta\vartheta$ [°]
T1	11.43	30.30	18.9
T2	11.38	30.24	18.9
T3	48.10	66.31	18.2
T4	52.48	80.53	28.1
T5	83.90	116.10	32.2
T6	95.49	114.76	18.8

The matching of the ΔE (vertical) strips to the E-detector vertical (front) strips

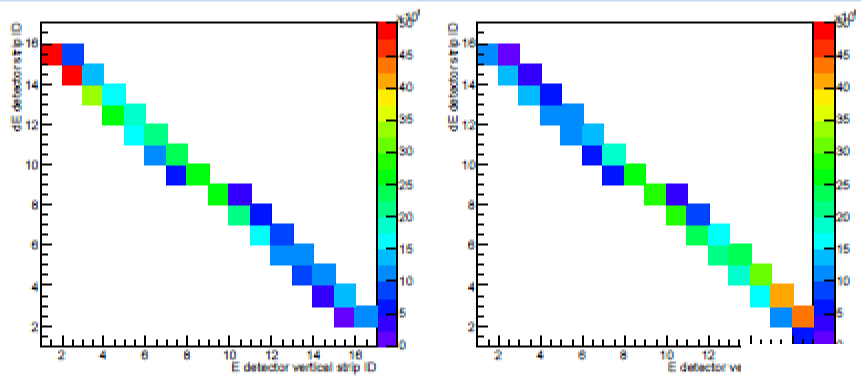

The ΔE-detector profiles for the T1 and T2.

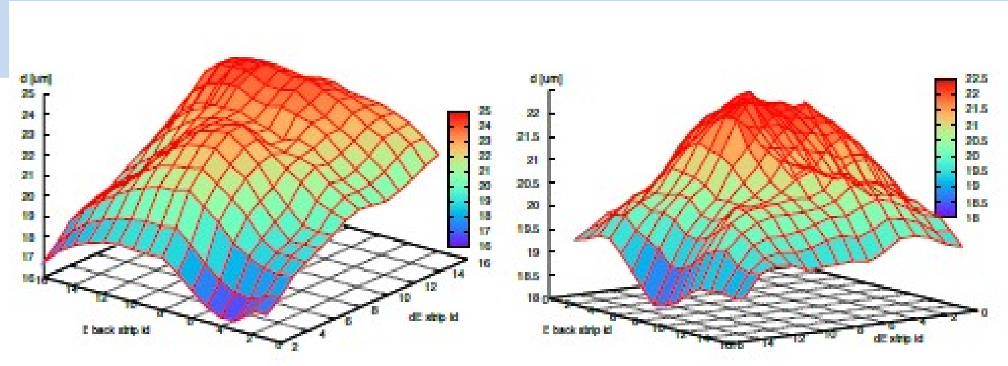

ΔE-E spectrum for the T1, ΔE-strip 13.

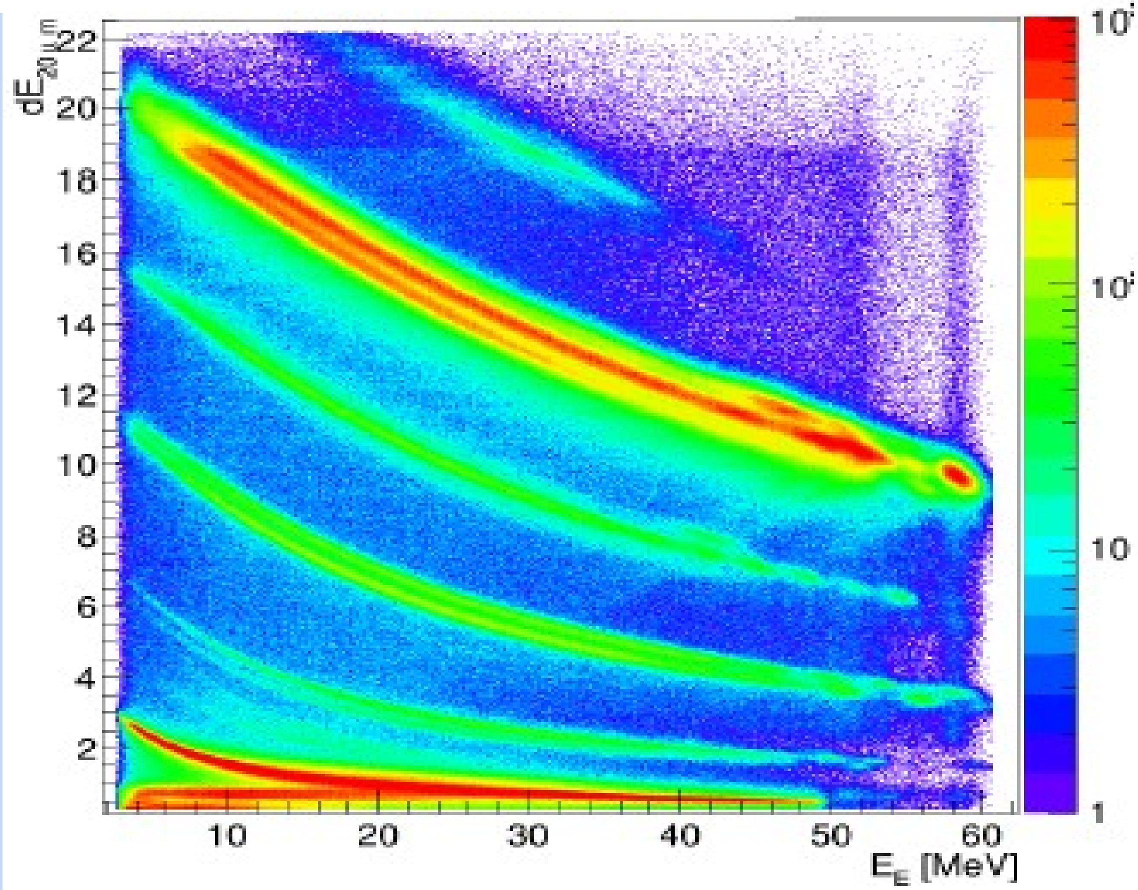

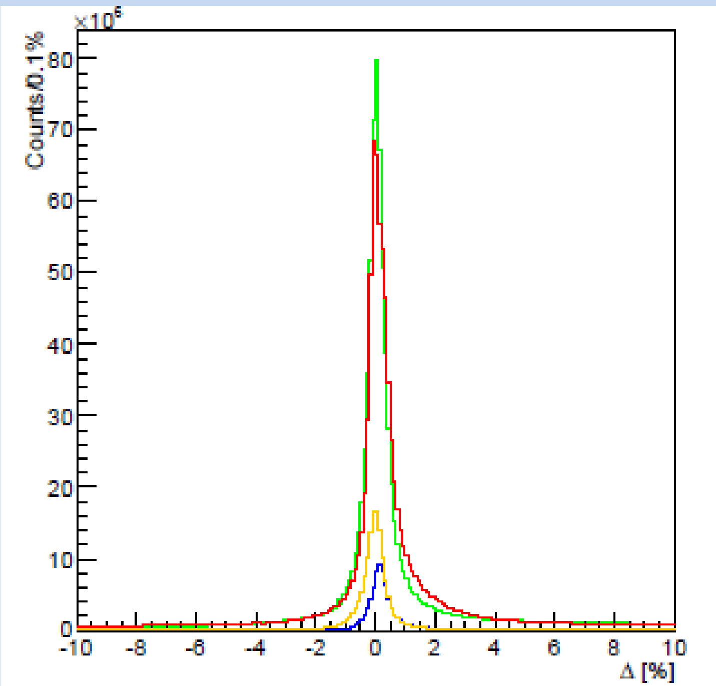

The front-strip vs back-strip energy difference relative to the average. Red line T1, green T2, blue T3, orange T4.

^{17}O results

^{9}Be+^{13}C→^{13}C+^{4}He+^{5}He reaction

^{13}C(T1)-^{4}He(T2), ^{13}C(T2)-^{4}He(T1), ^{13}C(T1)-^{4}He(T4) and ^{13}C(T2)-^{4}He(T3) coincident events

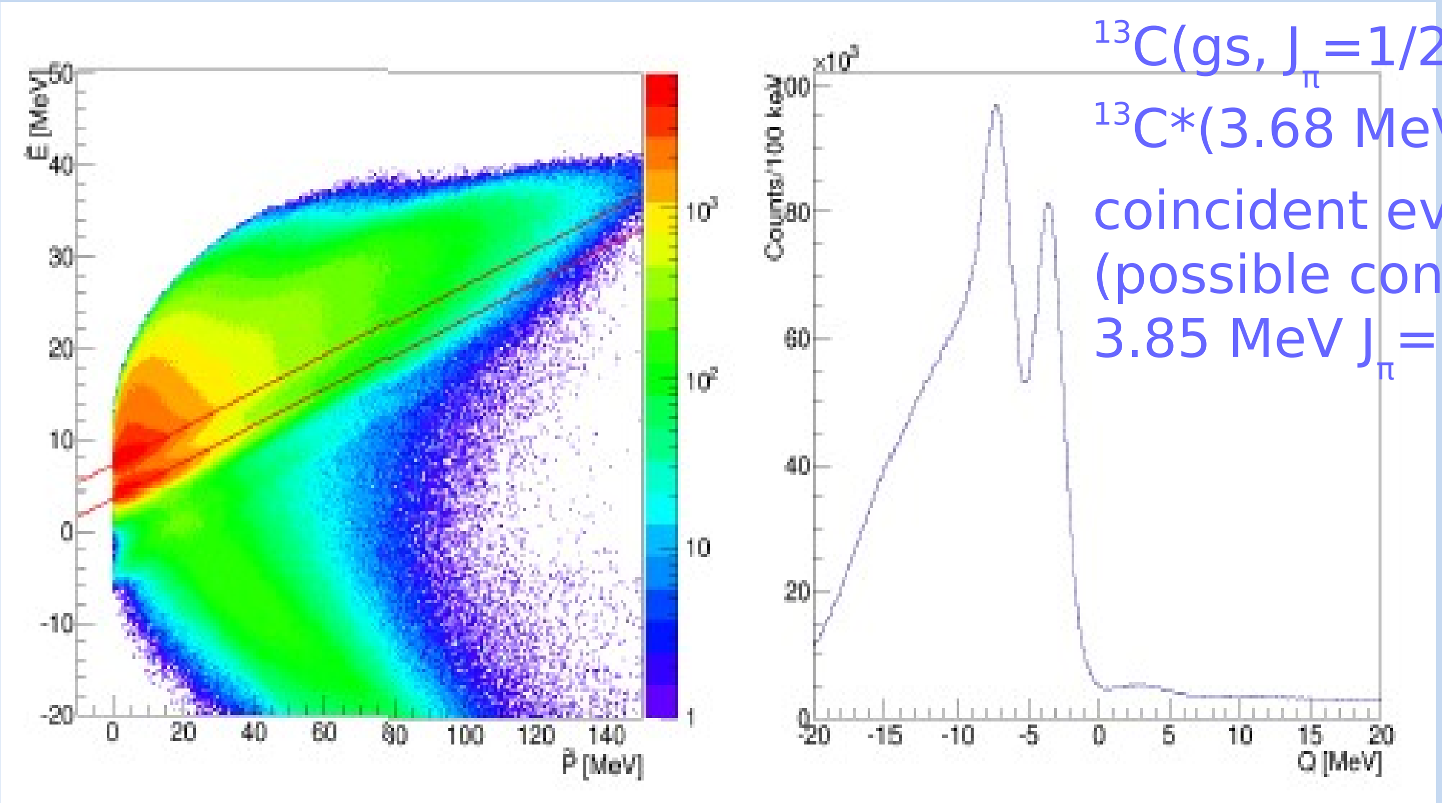

^{13}C(gs, $J_\pi=1/2^-$)+^{4}He and ^{13}C*(3.68 MeV, $J_\pi=3/2^-$)+^{4}He coincident events in T1-T2. (possible contribution of 3.85 MeV $J_\pi=5/2^+$)

Reaction identification: Catania plot

$\hat{E} = \mathcal{P}/A_3 - Q$, A_3 mass of undetected product

$\hat{E} = E_p - E_1 - E_2$

$\mathcal{P} = p_3^2/(2m_n)$

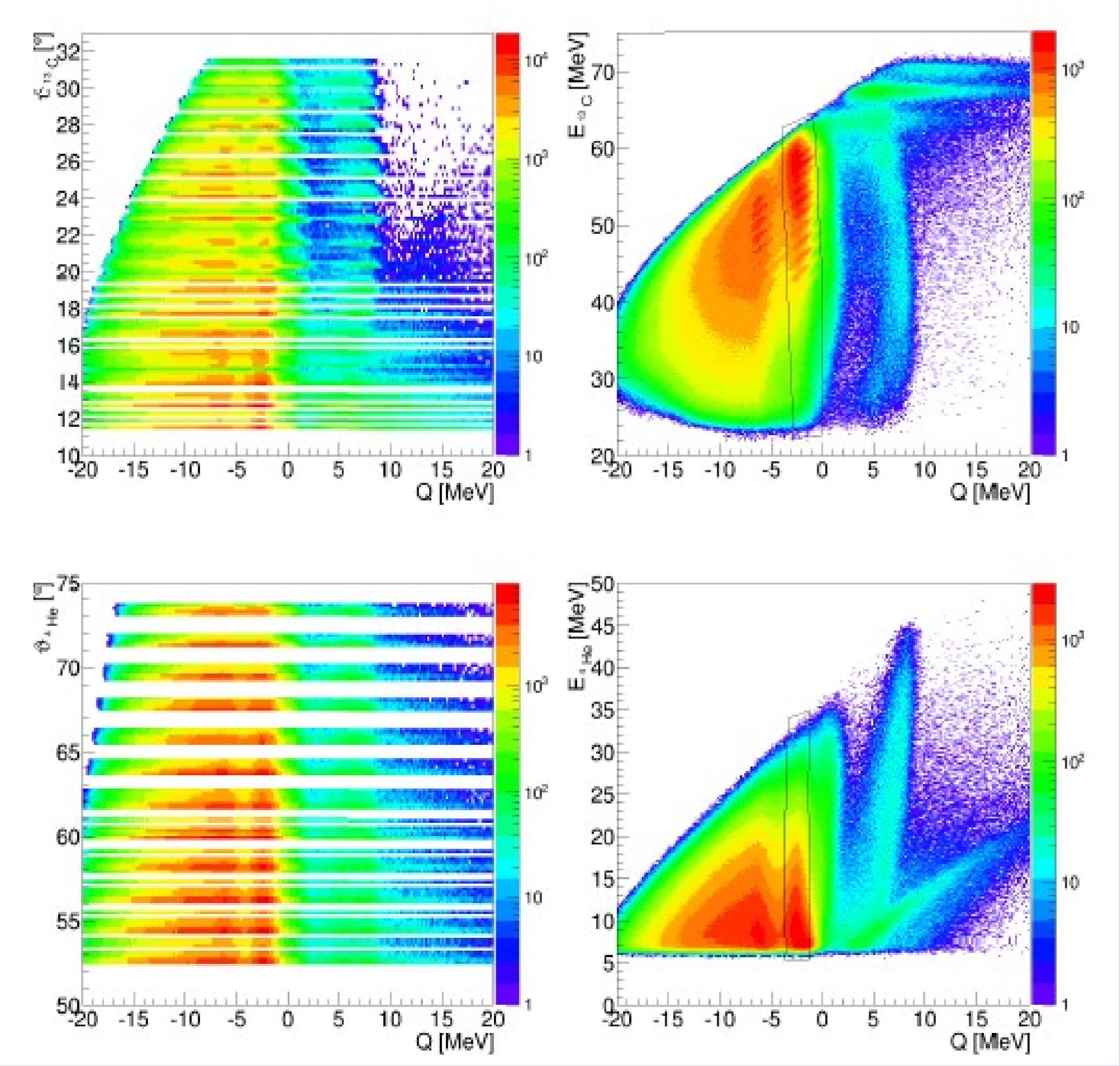

The Θ_{det}-Q and E_{det}-Q spectra for the ^{13}C(T1)-^{4}He(T4) coincident events. The black line denotes the graphical cuts used to select the ground state reaction channel.

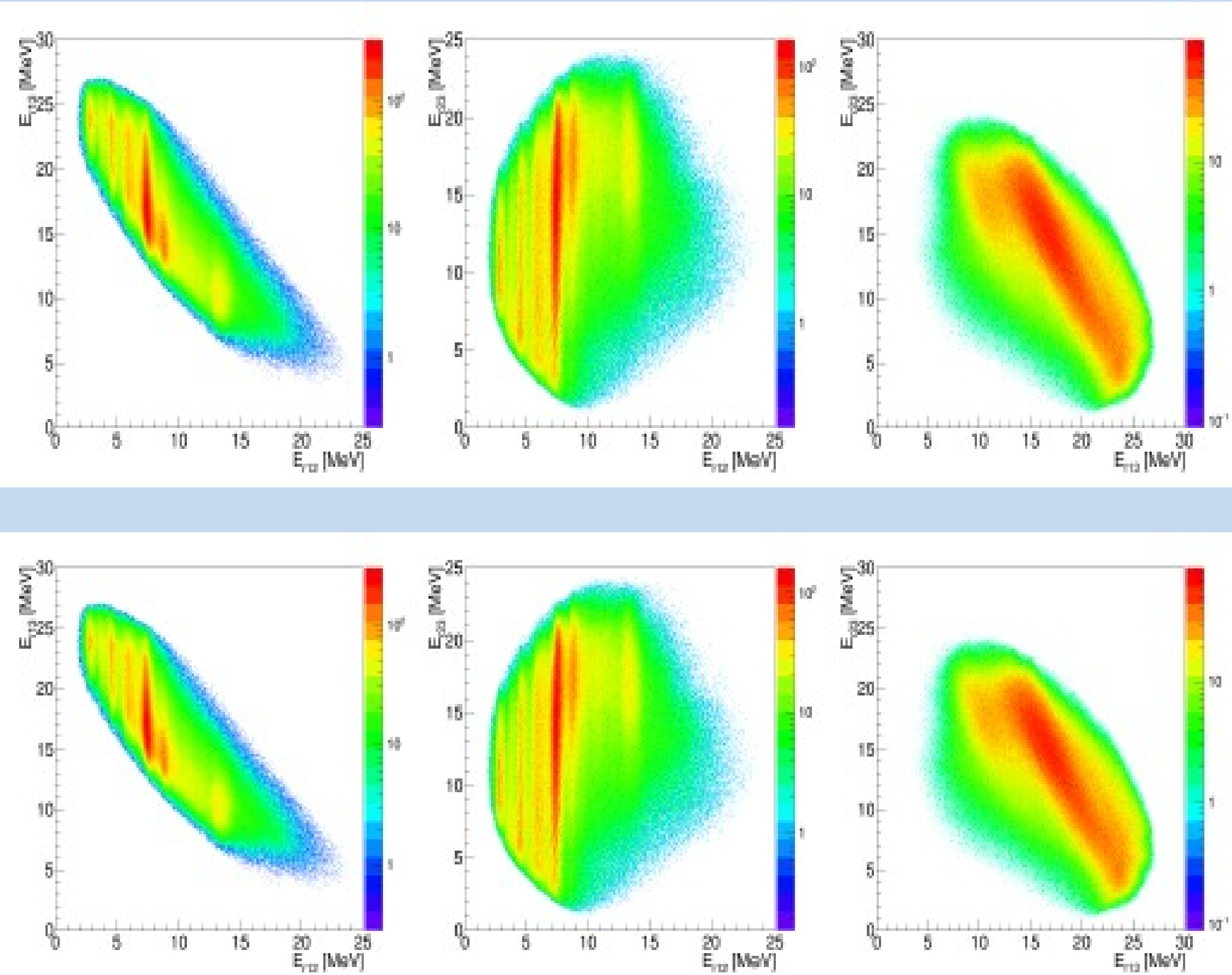

Exit channel $^{13}C+^{4}He+^{5}He$

$^{17}O=^{13}C+^{4}He$ T1-T2 events

$^{9}Be=^{4}He+^{5}He$ T1-T4, T2-T3 events

$^{18}O=^{13}C+^{5}He$ not observed

Relative-energy plots for the $^{9}Be(^{13}C,^{13}C^{4}He)^{5}He$ reaction. The ^{13}C(T1/T2), ^{4}He(T2/T1) and ^{5}He (undetected) are labeled by numbers 1, 2 and 3.

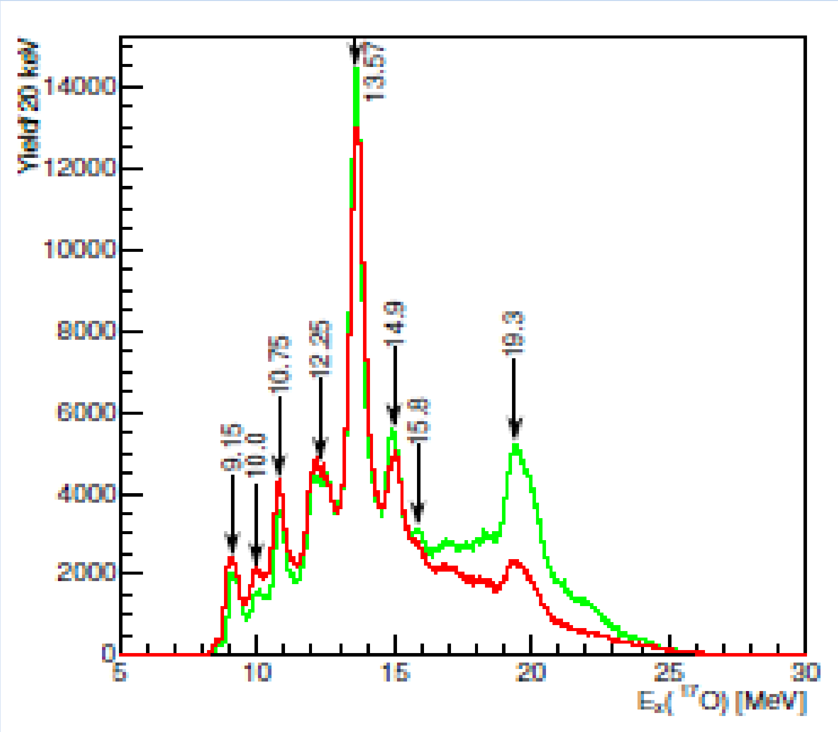

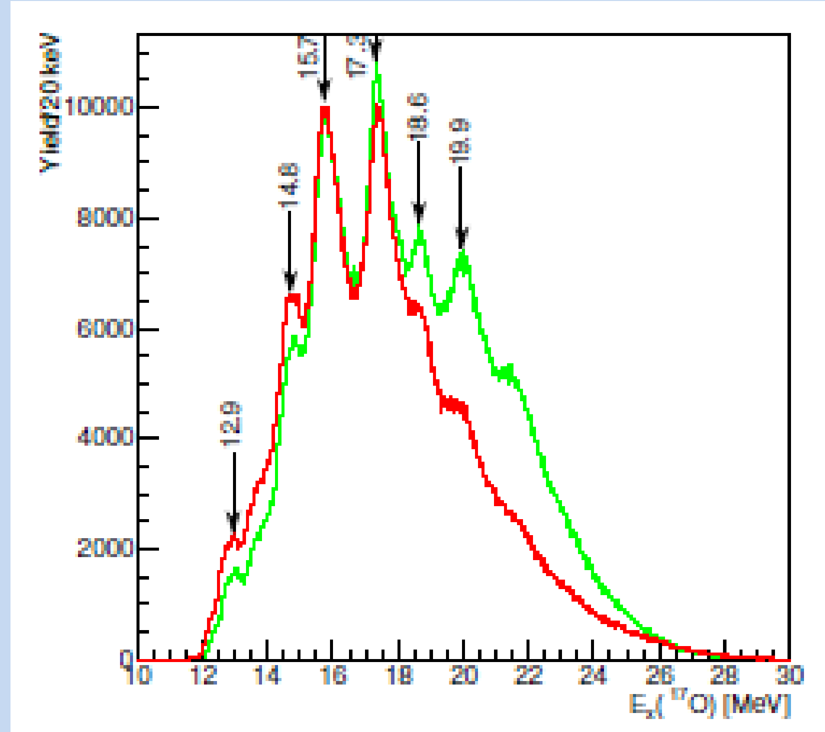

The ^{17}O excitation energy spectrum reconstructed from the $^{13}C(gs, J_\pi=1/2^-)+^4He$ coincident events in T1-T2 (red) and T2-T1 (green).

The ^{17}O excitation energy spectrum reconstructed from the $^{13}C^*(3.68\ MeV, J_\pi=3/2^-)+^4He$ coincident events in T1-T2 (red) and T2-T1 (green). (possible contribution 3.85 MeV $J_\pi=5/2^+$)

No.	$^{13}C+^{4}He$ res. el.		$^{13}C+^{9}Be$ reactions		References	Tilley *et. al.* [50]	
	E_x [MeV]	J^π	$^{13}C+^{4}He$ coinc.	$^{13}C^{*}+^{4}He$ coinc.		E_x [MeV]	J^π
1	8.9	$\left(\frac{7}{2}^-\right)$ or $\left(\frac{9}{2}^-\right)$			[7]		
2	9.2	$\left(\frac{7}{2}^-\right)$ or $\left(\frac{9}{2}^-\right)$	9.15		[5], [7], [98], [101], [102]	9.147	$\frac{1}{2}^-$
3	$10.0^{\dagger}$		10.0		[7]	9.976	$\frac{5}{2}^-$
4	$10.75^{\dagger}$		10.75		[6], [100], [101]	10.777	$\frac{1}{2}^+, \frac{7}{2}^-$
5	12.0	$\left(\frac{11}{2}^+\right)$ or $\left(\frac{13}{2}^-\right)$	12.25 (wide)		[61], [96], [97], [98]	12.005 ± 15	$> \frac{3}{2}$
6	12.8			12.9	[100]	12.93	
7	13.6	$\left(\frac{11}{2}^-\right)$	**13.57**		[4], [5], [98], [100]	13.58	$(\frac{11}{2}, \frac{13}{2})^-$
8			14.9	14.8	[4], [6], [100]	15.1 ± 0.1	$\left(\frac{9}{2}^+, \frac{11}{2}^+\right)$
9			15.8	**15.7**	[4], [6]*, [100], [103],	15.95	$\left(\frac{9}{2}^+, \frac{11}{2}^+\right)$
10			(weak peak)	**17.3**	[3], [6]*, [98], [105]	17.06	$\frac{11}{2}^-$
11			(weak peak)	18.6	[6]*	18.72	
12			19.3		[6], [4], [104]		
13				19.6	[3], [6]*	19.6	$\left(\frac{13}{2}^+, \frac{15}{2}^+\right)$

Published results:

(6) M. Milin et al, EPJ A 41 (2009) 335, the same reaction

(7) M. Heil et al, PRC 78 (2008) 025803, the $^{13}C+^{4}He$ thick target resonant scattering up to excitation 11.1 MeV

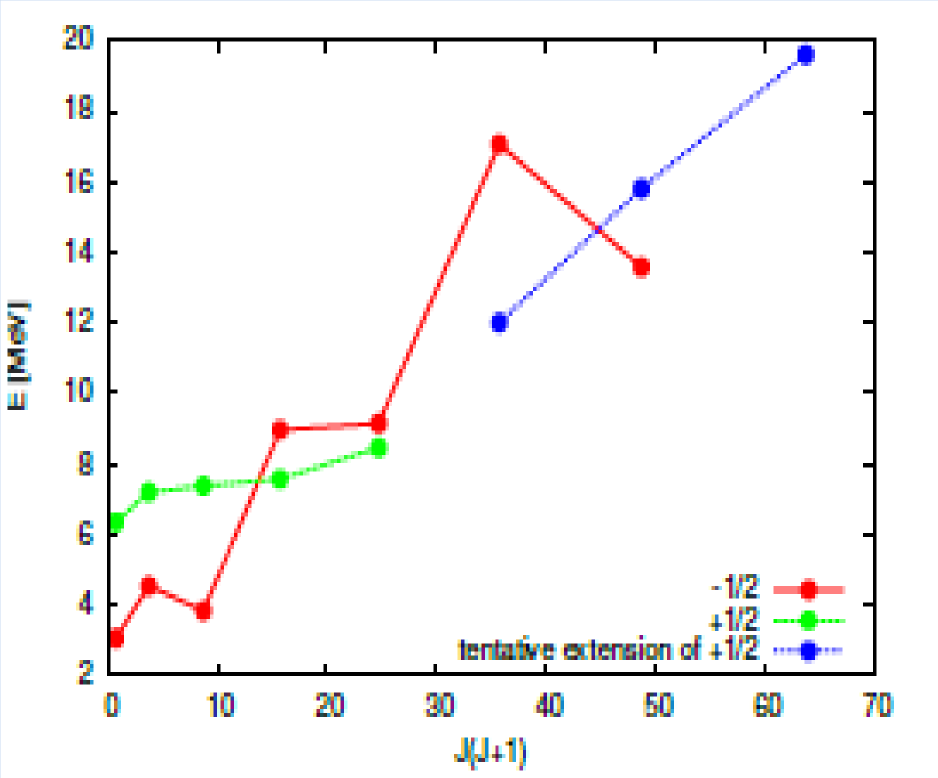

A tentative extension of the proposed ^{17}O positive-parity rotational band and the negative-parity rotational band [6].

^{18}O results

$^{9}Be+^{13}C\rightarrow^{4}He+^{18}O^{*}\rightarrow$

$^{14}C+^{4}He+^{4}He$, $^{14}C^{*}(E_{x}\approx 7$ MeV $0^{-},2^{+},2^{-})+^{4}He+^{4}He$

$^{12}C+^{6}He+^{4}He$, $^{12}C^{*}(E^{x}=4.4$MeV $2^{+})+^{6}He+^{4}He$

$^{10}Be+^{8}Be+^{4}He$, $^{10}Be^{*}+^{8}Be+^{4}He$ ($E_{x}=3.37$MeV 2^{+};≈ 6.2 MeV $2^{+},1^{-},0^{+},2^{-}$)

Events for all possible telescope combinations

^{14}C(T1)-^{4}He(T2)

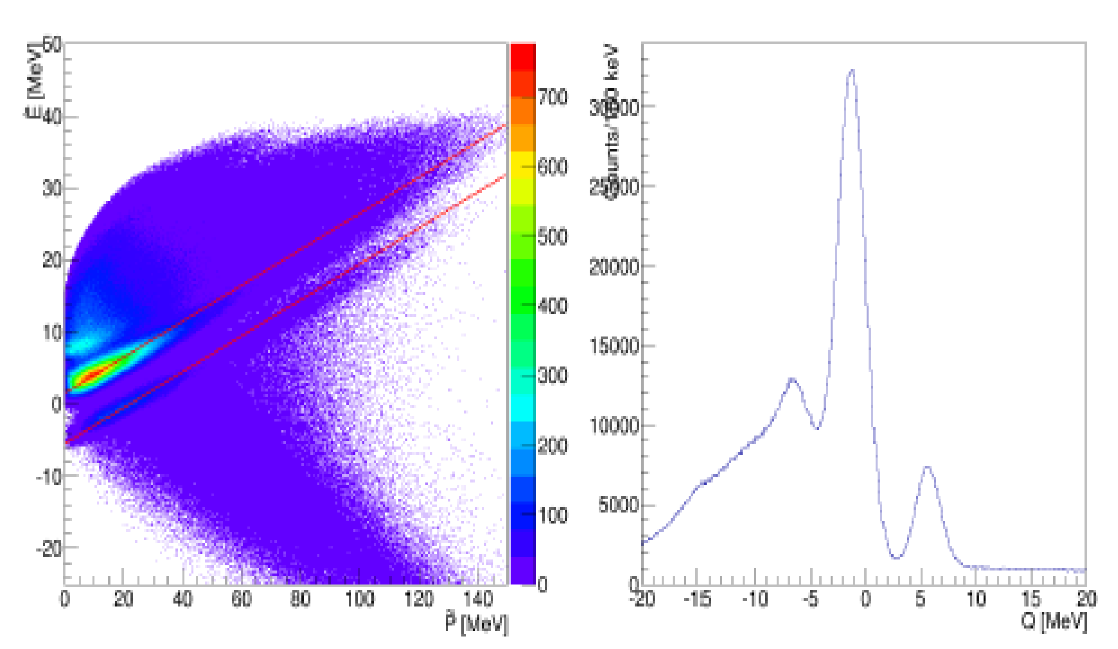

^{14}C(gs, $J^{\pi}=0^{+}$)+^{4}He and $^{14}C^{*}$(7 MeV)+^{4}He in T1-T2

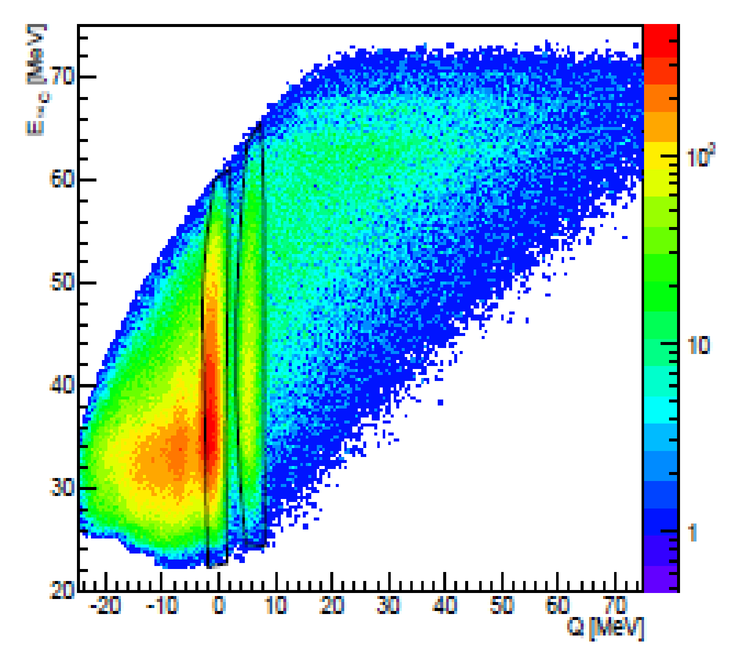

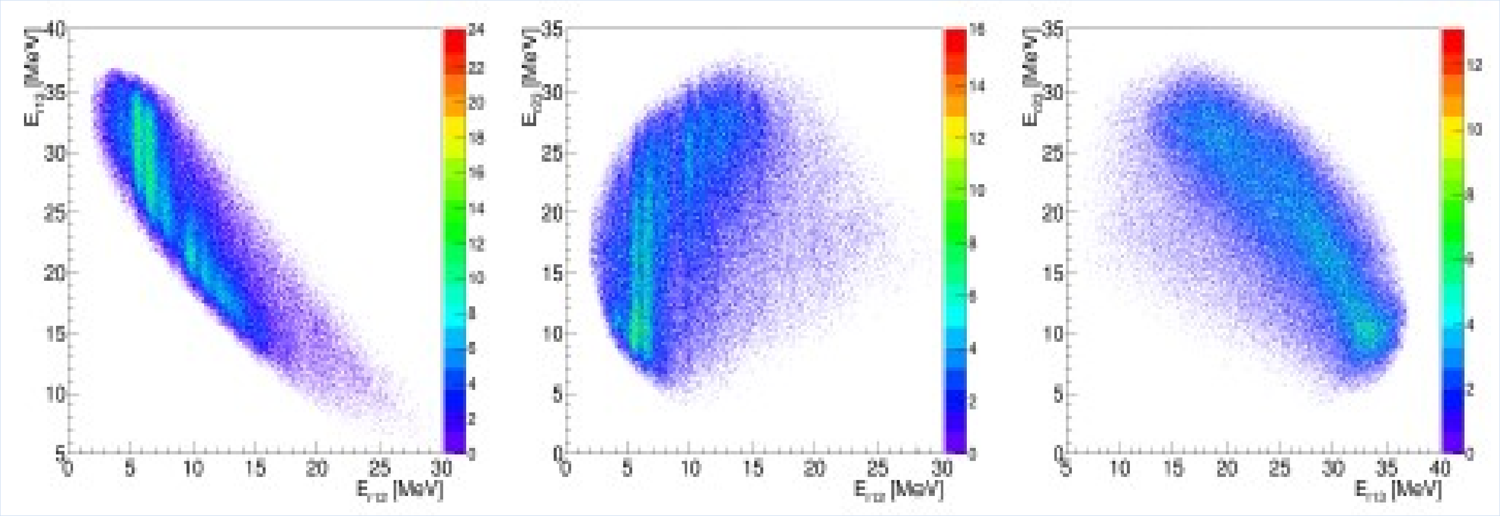

Relative-energy plots for the $^{9}Be(^{13}C,^{14}C^{4}He)^{4}He$ reaction. The ^{14}C(T1), ^{4}He(T2) and ^{4}He (undetected) are labeled by numbers 1, 2 and 3.

graphical cuts

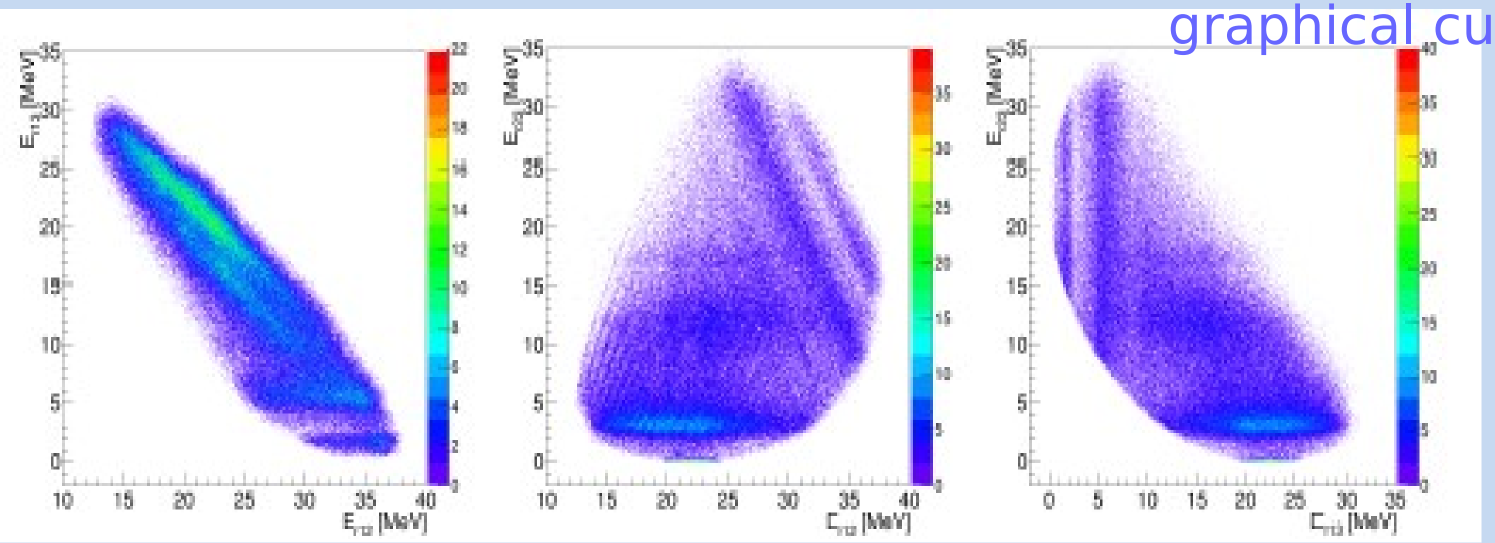

Relative-energy plots for the $^{9}Be(^{13}C,^{14}C^{4}He)^{4}He$ reaction. The ^{14}C(T1), ^{4}He(T4) and ^{4}He (undetected) are labeled by numbers 1, 2 and 3.

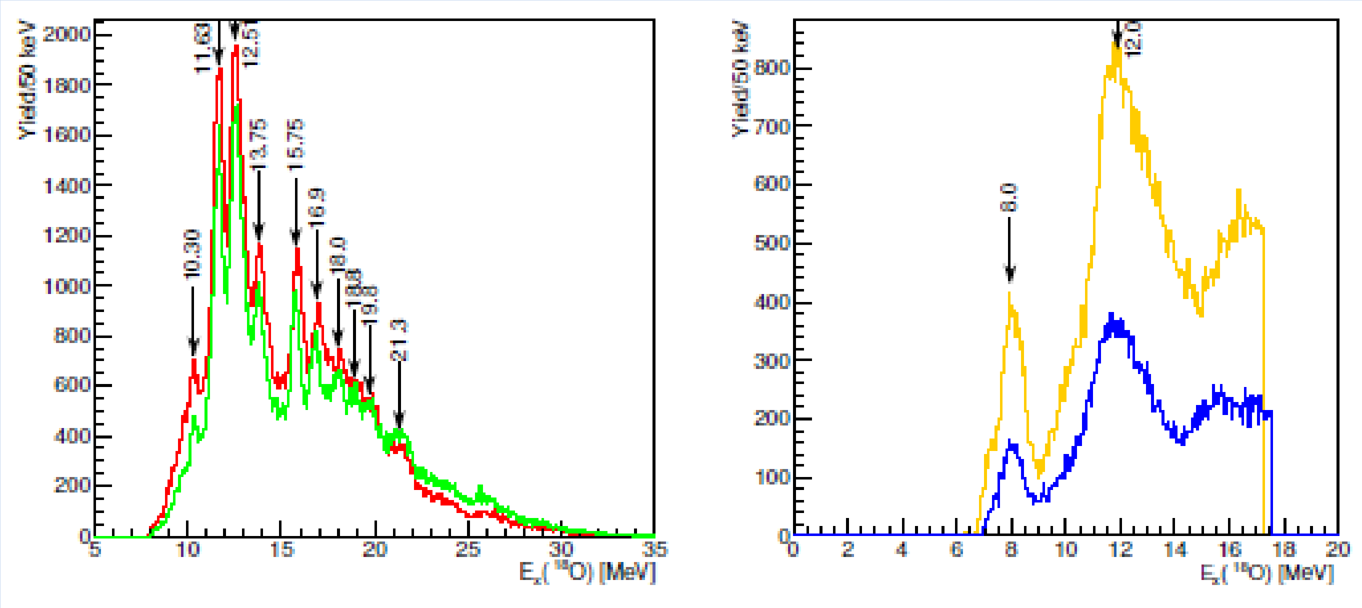

The ^{18}O excitation energy spectrum for the $^{14}C(gs)+^{4}He$ coincident events in T1-T2 (red), T2-T1 (green), T1-T4 (orange) and T2-T3 (blue).

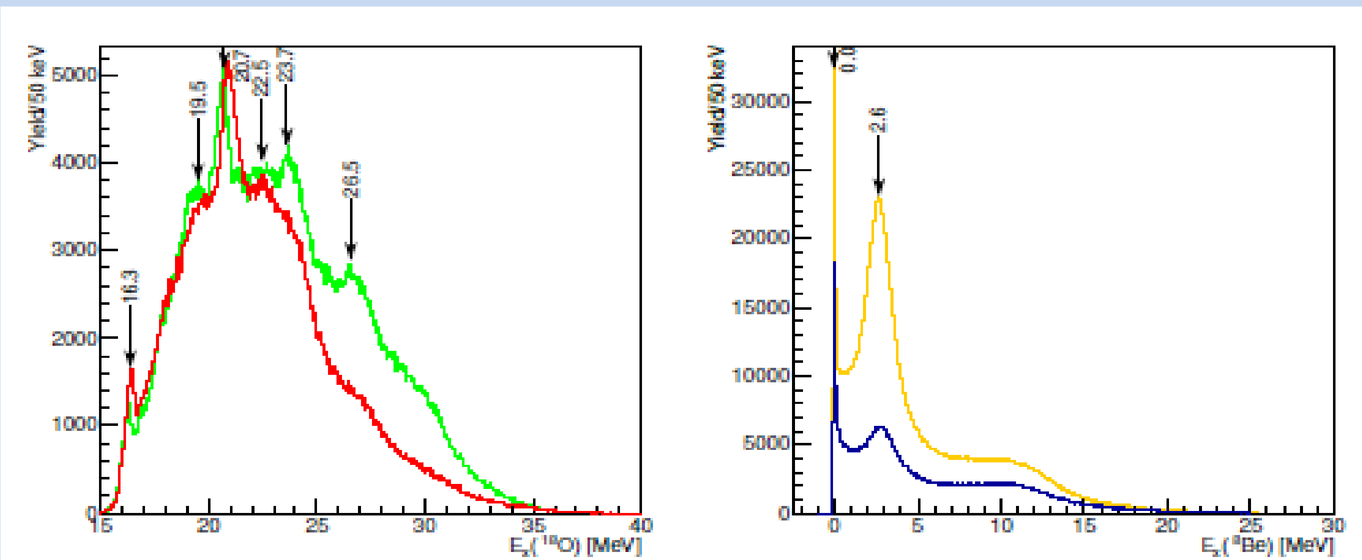

The ^{18}O excitation energy spectrum for the $^{14}C^{*}(7\ MeV)+^{4}He$ events in T1-T2 (red) and T2-T1 (green); ^{8}Be spectrum for T1-T4 (orange) and T2-T3 (blue).

$^{9}Be+^{13}C \rightarrow ^{12}C+^{6}He+^{4}He$ reaction

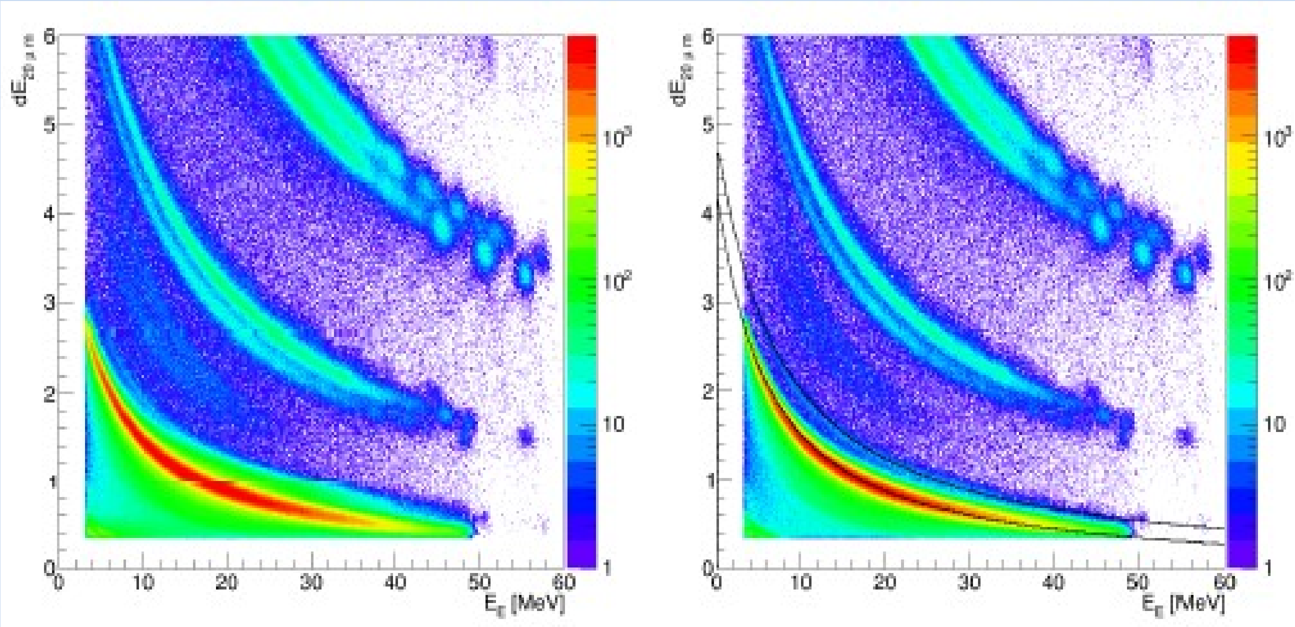

Additional ΔE-E spectra filtering to separate ^{6}He from ^{4}He for the T1, ΔE-strip 8. Black lines show results of simulations for $^{4,6}He$ in T1

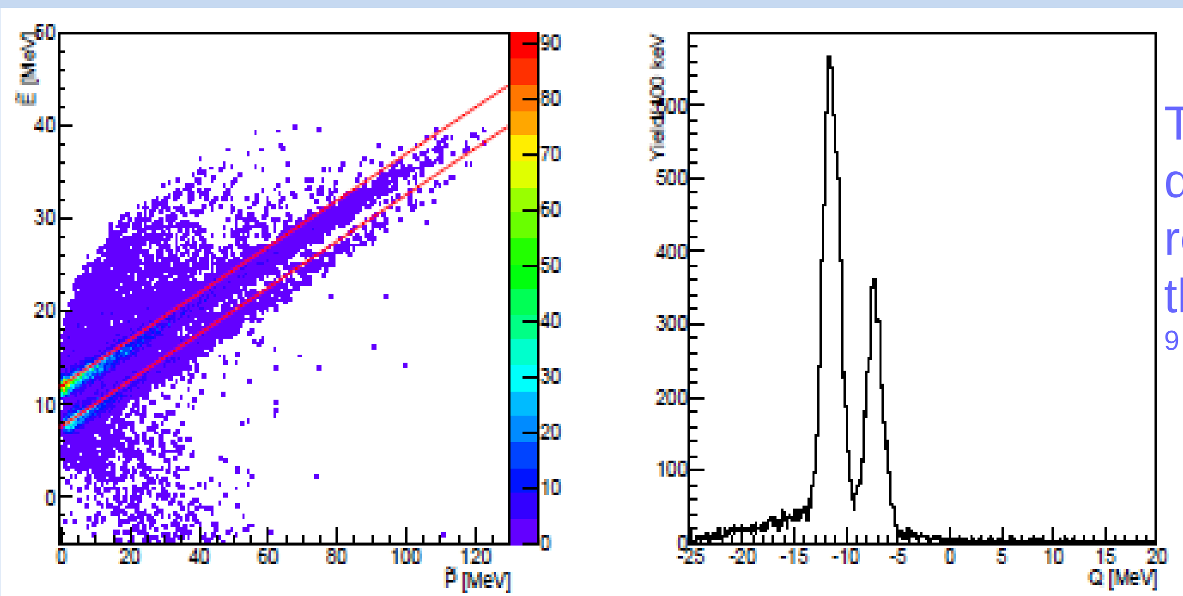

The Catania plot for the ^{6}He detected in T1 and ^{12}C in T2. The red lines are predicted loci for the $^{9}Be(^{13}C,^{6}He^{12}C(gs))^{4}He$ and $^{9}Be(^{13}C,^{6}He^{12}C^{*}(4.4\ MeV))^{4}He$.

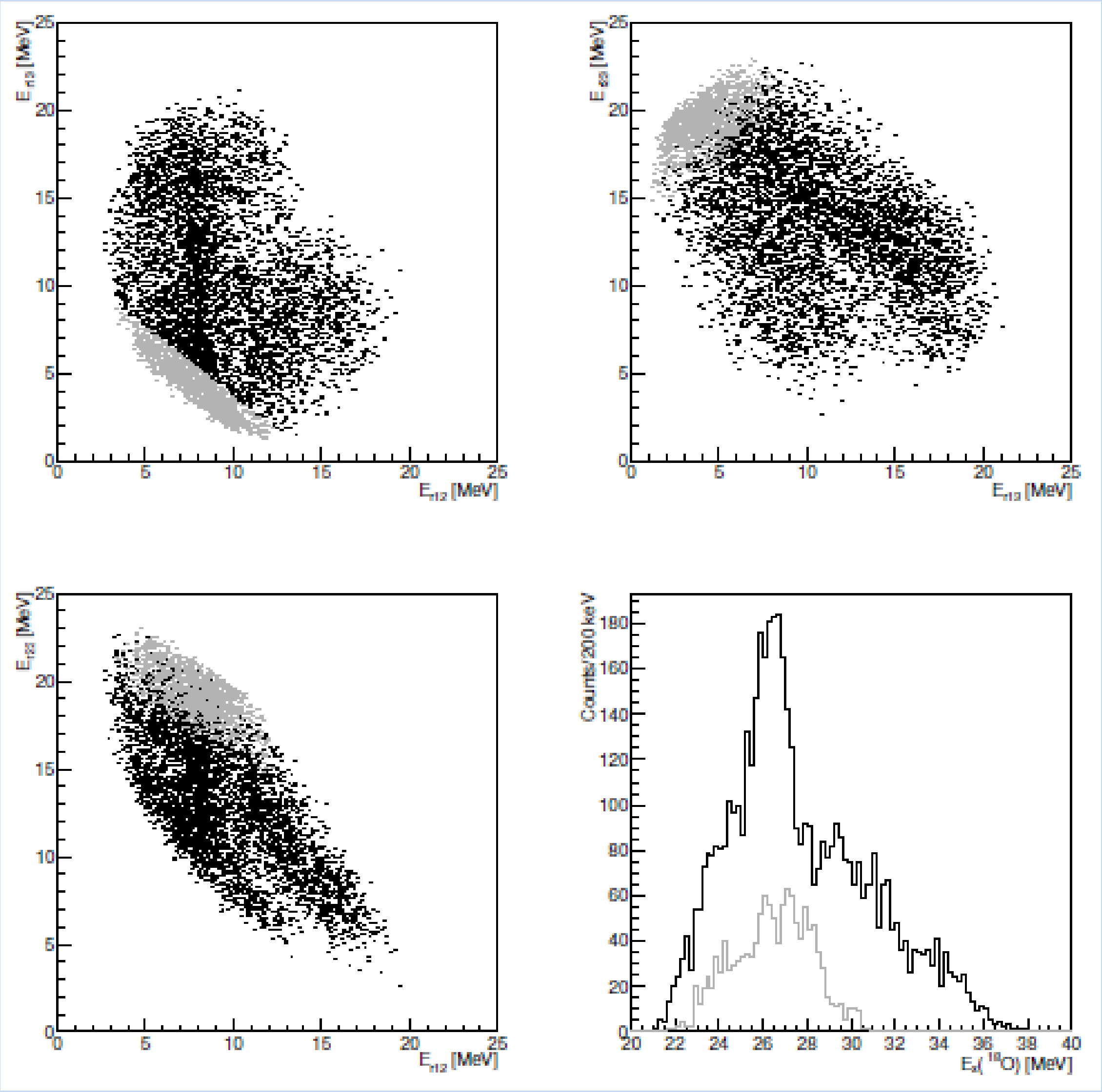

broad peak at 26.5 MeV, indications of peaks at 29.5 MeV and around 23.5 MeV.

E_r-E_r plots for ^{6}He and ^{12}C(gs) detected in T1 and T2, labelled as 1 and 2. The last plot is the ^{18}O excitation energy spectrum for events selected via graphical cut (black dots). The grey dots correspond to events from the ^{16}O decay. For the ^{12}C*(4.4 MeV) +^{6}He events excitation spectrum is structureless.

No.	$E_x(^{18}O)$ from the $^{13}C+^{9}Be$ reactions			References	Tilley *et. al.* [87]	
1	$^{14}C+^{4}He$	$^{14}C^{*}+^{4}He$	$^{12}C+^{6}He$		E_x [MeV]	J^{π}
2	10.30 MeV			[12], [13], [14], [106], [107], [108], [109], [110], [111], [112], [113], [114]	10.290 MeV	4^+
3	**11.63 MeV**			[12], [13], [14], [101], [106], [107], [108], [109], [111], [113]	11.62 MeV	5^-
4	**12.51 MeV**			[12], [13], [14], [106], [107], [108], [109], [111]	12.53 MeV	6^+
5	**13.75 MeV**			[111]	13.8	1^-
6				[13], [14]	13.82	5^-
7	15.75 MeV			[111]	15.8	1^-
8		**16.1 MeV**		[12]	16.315	$(3,2)^-$
9	16.9 MeV			[107], [109]	16.948	$(2,3)^-$
10	18.0 MeV			[115]	18.049	
11	18.8 MeV			[110], [115]	18.68	(4^-)
12		19.3 MeV				
13	19.8 MeV					
14		**20.5 MeV**		[110]	20.86	
15	21.3 MeV			[110], [117]	21.42	(4^-)
16		22.3 MeV		[110]	22.4	4^-
17		23.5 MeV	23.5 MeV	[110], [116]	23.8	1^-
18		26.3 MeV	26.5 MeV	[116]	27	1^-
19			29.5 MeV	[116]	30	

Published many results, some recent:

(14) M. L. Avila et al, PRC 90 (2014) 024327, the $^{14}C+^{4}He$ thick target resonant scattering

(12) N. Curtis et al, PRC 66 (2002) 024315, $^{14}C(^{18}O,^{14}C\,^{4}He)^{14}C$

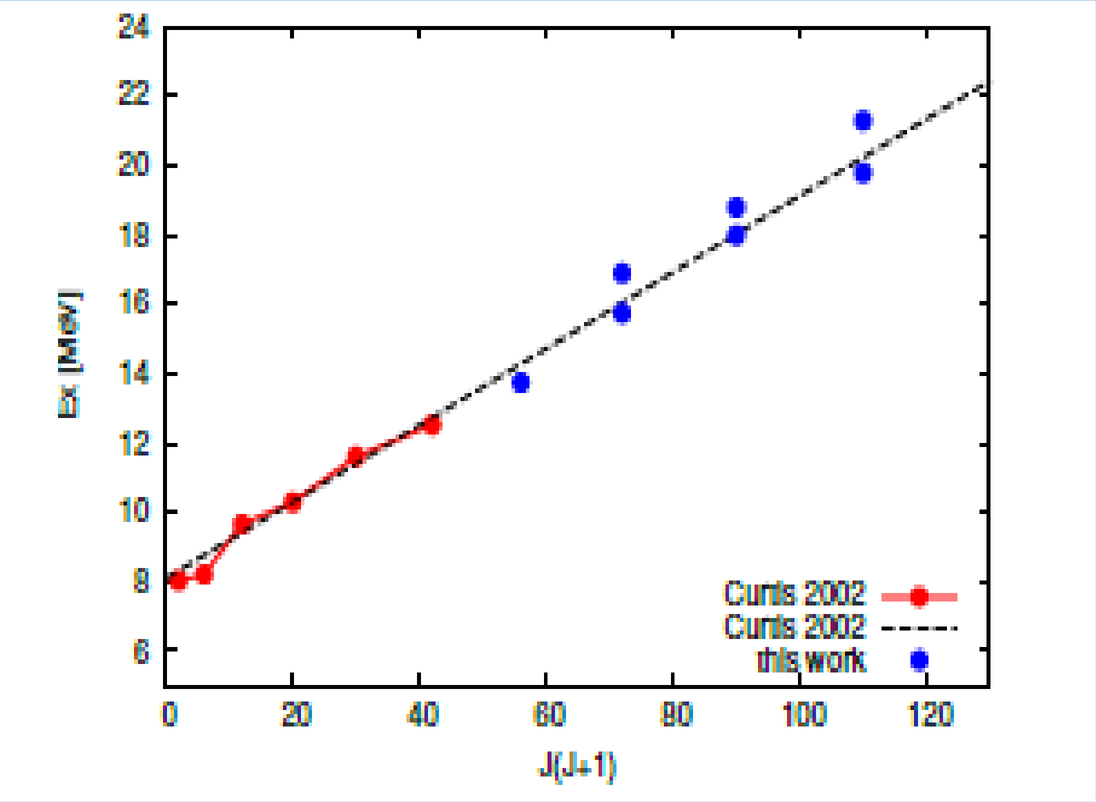

A tentative extension of the proposed ^{18}O rotational band [12].
In agreement with proposed rotational bands in W. von Oertzen et al, EPJ A 43 (2009) 17

Conclusion of Ref. [14] is that the α-strength is typically not concentrated in one state, but spread among multiple states, making such rotational bands unlikely.

Summary & outlook

- the resonant scattering $^{13}C+^{4}He$ experiment and resonant particle spectroscopy experiment with the $^{13}C+^{9}Be$ reaction populated excited states with cluster structure in the ^{17}O and ^{18}O (RPSE)
- existing results on the ^{4}He decays confirmed and extended
- the ^{6}He decaying states in ^{18}O have been observed for the first time – the first indication of the molecular structure
- these measurements should be complemented with other technique experiments, for example thick target resonant scattering measurements
- further measurements using different techniques are needed to determine the exact value of spin and parity, with higher resolution and statistics to separate nearby states
- there are strong indications that molecular structure exist in oxygen isotopes but much more experimental dana are required

Thank you !